

# Beyond maps: Patterns of formation processes at the Middle Pleistocene open-air site of Marathousa 1, Megalopolis Basin, Greece

D. Giusti<sup>a,\*</sup>, V. Tourloukis<sup>a</sup>, G. E. Konidaris<sup>a</sup>, N. Thompson<sup>b</sup>, P. Karkanas<sup>c</sup>, E. Panagopoulou<sup>d</sup>, K. Harvati<sup>a</sup>

<sup>a</sup>*Paläoanthropologie, Senckenberg Centre for Human Evolution and Palaeoenvironment, Eberhard Karls Universität Tübingen, Rümelinstr. 23, 72070 Tübingen, Germany*

<sup>b</sup>*Friedrich-Alexander University of Erlangen-Nürnberg, Institute of Prehistory and Early History, Kochstr. 4/18, 90154 Erlangen, Germany*

<sup>c</sup>*Malcolm H. Wiener Laboratory for Archaeological Science, American School of Classical Studies at Athens, Greece*

<sup>d</sup>*Ephoreia of Palaeoanthropology-Speleology of Greece, Athens, Greece*

---

## Abstract

Recent excavations at the Middle Pleistocene open-air site of Marathousa 1 have unearthed in one of the two investigated area (Area A) a partial skeleton of a single individual of *Elephas (Palaeoloxodon) antiquus* and other faunal remains in spatial and stratigraphic association with lithic artefacts. In Area B, a much higher number of lithic artefacts was collected, spatially and stratigraphically associated with other faunal remains. The two areas are stratigraphically correlated, the main fossiliferous layers representing an *en masse* depositional process in a lake margin context. Evidence of butchering (cut-marks) has been identified on two bones of the elephant skeleton, as well on other mammal bones from Area B. However, due to the secondary deposition nature of the main find-bearing units, it is of primary importance to evaluate the degree and reliability of the spatial association of the lithic artefacts with the faunal remains. Indeed, spatial association does not necessarily imply causation. The present study uses a comprehensive set of multiscale and multivariate spatial statistics, in order to disentangle the depositional processes behind the distribution of the archaeological and palaeontological record at Marathousa 1. Moving beyond distribution maps,

---

\*Corresponding author

Email address: domenico.giusti@uni-tuebingen.de (D. Giusti)

statistical inference allows for a better interpretation of spatial patterns by adopting a more inductive and reproducible strategy. Moreover, within a frame of references, it enables us to depict the underlying processes responsible for the observed patterns, and to quantify the extent of the post-depositional reworking processes which have long been recognised to affect the integrity of archaeological assemblages. Assessing the degree of disturbance is crucial to fully comprehend the archaeological record, and therefore to reliably interpret past human behaviours. Preliminary results of our analyses suggest minor reworking and substantial spatial association of the lithic and faunal assemblages, supporting the current interpretation of Marathousa 1 as a butchering site.

*Keywords:* Spatial taphonomy, Vertical distribution, Fabric analysis, Point pattern analysis, Site formation processes, Middle Pleistocene

---

## **1. Introduction**

The analysis of archaeological site formation and modification processes, intensively studied since the early 1970s (Isaac, 1967; Schiffer, 1972, 1983, 1987; Shackley, 1978; Wood and Johnson, 1978; Schick, 1984, 1986, 1987; Petraglia and Nash, 1987; Petraglia and Potts, 1994, among others), is nowadays fully integrated in the archaeological practice. Drawing inferences about past human behaviours from scatters of archaeological remains must account for depositional and post-depositional contextual processes.

Several methods are currently applied in order to qualify and quantify the type and degree of reworking of archaeological assemblages. Within the framework of a geoarchaeological and taphonomic approach, spatial statistics offer meaningful contributions in unravelling site formation and modification processes from spatial patterns.

The study of the clast fabric (dip and strike of elongated sedimentary particles, including bones and artefacts), first addressed by Isaac (1967); Bar-Yosef and Tchernov (1972); Schick (1986), has more recently been found to successfully discriminate between sedimentary processes (Bertran and Texier, 1995; Bertran et al., 1997), leading to a noteworthy development of methods and propagation of applications in Palaeolithic site formation studies (Lenoble and Bertran, 2004; Lenoble et al., 2008; McPherron,

19 2005; Benito-Calvo et al., 2009; Benito-Calvo and de la Torre, 2011; Benito-Calvo  
20 et al., 2011; Bernatchez, 2010; Domínguez-Rodrigo et al., 2012; García-Moreno et al.,  
21 2016; Sánchez-Romero et al., 2016, among others).

22 The vertical distribution of materials, on the other hand, has been long investigated  
23 with the aim of identifying cultural levels, by visually interpreting virtual profiles (but  
24 see Anderson and Burke (2008) for a quantitative approach).

25 However, archaeological horizons may be subject to vertical rearrangement by syn-  
26 and post-depositional processes. Several experimental studies have investigated the  
27 effect of trampling on the vertical displacement of artefacts (Villa and Courtin, 1983;  
28 Gifford-Gonzalez et al., 1985; Nielsen, 1991; Eren et al., 2010). Although these works  
29 have reported a negative correlation between artefact size and vertical displacement,  
30 particle size sorting of lithic assemblages, when exposed to physical geomorphic agents  
31 (such as gravity, water flow, waves and tides, wind), has been widely documented  
32 (Rick, 1976; Schick, 1986; Petraglia and Nash, 1987; Morton, 2004; Lenoble, 2005;  
33 Bertran et al., 2012).

34 Bone and lithic refitting analysis is an additional, particularly robust method in  
35 investigating the stratigraphic integrity of a site (Villa, 1982, 1990; Todd and Stanford,  
36 1992; Morin et al., 2005; Sisk and Shea, 2008). Furthermore, lithic refits have been  
37 shown to provide reliable clues about the spatio-temporal dimension of past human  
38 behaviours, by discriminating activity areas (López-Ortega et al., 2011, 2015; Vaquero  
39 et al., 2012, 2015; Clark, 2016).

40 Finally, distribution maps are cornerstones of the archaeological documentation  
41 process and are primary analytic tools. However, their visual interpretation is prone  
42 to subjectivity and is not reproducible. Since the early 1970's (see Hodder and Or-  
43 ton (1976); Orton (1982) and references therein), the traditional, intuitive, 'eyeballing'  
44 method of spotting spatial patterns has been abandoned in favour of more objective ap-  
45 proaches, extensively borrowed from other fields. Nevertheless, quantitative methods,  
46 while still percolating in the archaeological sciences from neighbouring disciplines, are  
47 not extensively used. Moreover, only a relatively small number of studies have explic-  
48 itly applied spatial point pattern analysis or geostatistics to the study of site formation  
49 and modification processes (Lenoble et al., 2008; Domínguez-Rodrigo et al., 2014b,a,

50      2017; Carrer, 2015; Giusti and Arzarello, 2016; Organista et al., 2017, but see Hivernel  
51      and Hodder (1984) for an earlier work on the subject).

52      The goal of a taphonomic approach to spatial analysis is to move beyond distribution  
53      maps by applying a comprehensive set of multiscale and multivariate spatial statistics,  
54      in order to reliably infer processes from spatial patterns. An exhaustive spatial analytic  
55      approach to archaeological inference, combined with a taphonomic perspective,  
56      is essential for the evaluation of the integrity of the archaeological assemblage, and  
57      consequently for a reliable interpretation of past human behaviours.

58      **2. Marathousa 1**

59      The object of the present study is the spatial distribution of the archaeological and  
60      palaeontological record recovered during excavation at the Middle Pleistocene open-air  
61      site of Marathousa 1, Megalopolis, Greece (Panagopoulou et al., 2015; Harvati et al.,  
62      2016).

63      The site (Fig. 1), discovered in 2013 at the edge of an active lignite quarry, is located  
64      between lignite seams II and III in the Pleistocene deposit of the Megalopolis basin,  
65      Marathousa Member of the Choremi Formation (van Vugt et al., 2000). The regular  
66      alternation of lacustrine clay, silt and sand beds with lignite seams has been interpreted  
67      having cyclic glacial (or stadial) and interglacial (or interstadial) origin (Nickel et al.,  
68      1996). The half-graben configuration of the basin, with major subsidence along the  
69      NE-SW trending normal faults at the eastern margin, resulted in the gentle dip of the  
70      lake bottom at the opposite, western, margin of the lake, enabling the formation of  
71      swamps and the accumulation of organic material for prolonged periods of time (van  
72      Vugt et al., 2000).

73      Two excavation areas have been investigated since 2013: Area A, where several  
74      skeletal elements of a single individual of *Elephas (Palaeoloxodon) antiquus* have been  
75      unearthed, together with a number of lithic artefacts (Konidaris et al., this volume;  
76      Tourloukis et al., this volume); and Area B, about 60 m to the South along the exposed  
77      section, where the lithic assemblage is richer and occurs in association with a faunal as-  
78      semblage composed by isolated elephant bones, cervids and carnivores among others.

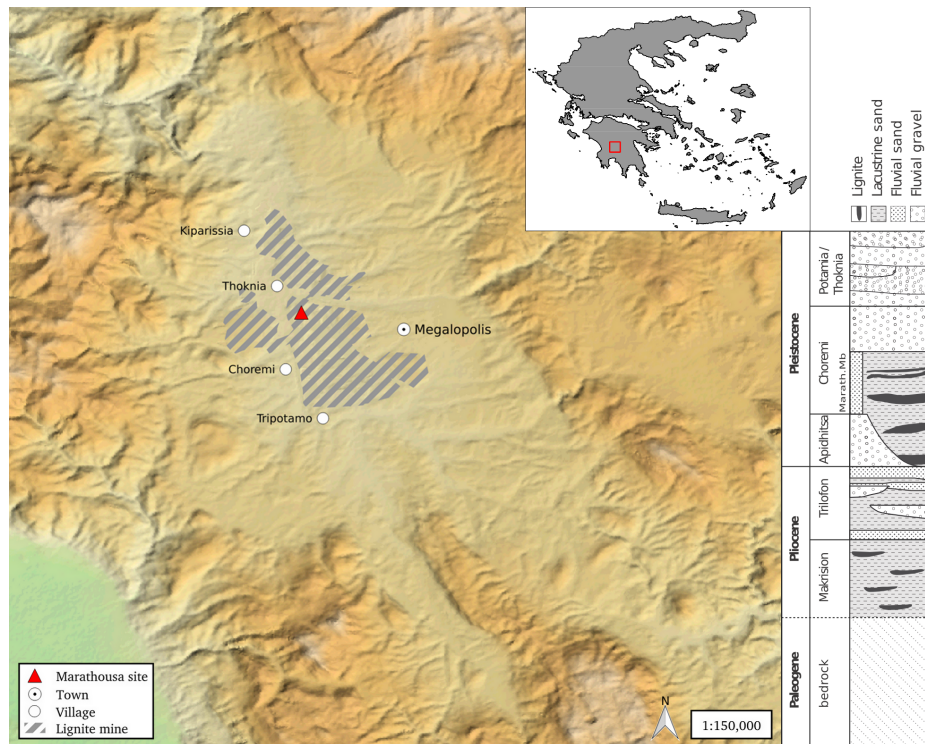


Figure 1: Geographical location of the Marathousa 1 site in the Megalopolis basin and stratigraphic column, modified after [van Vugt et al. \(2000\)](#).

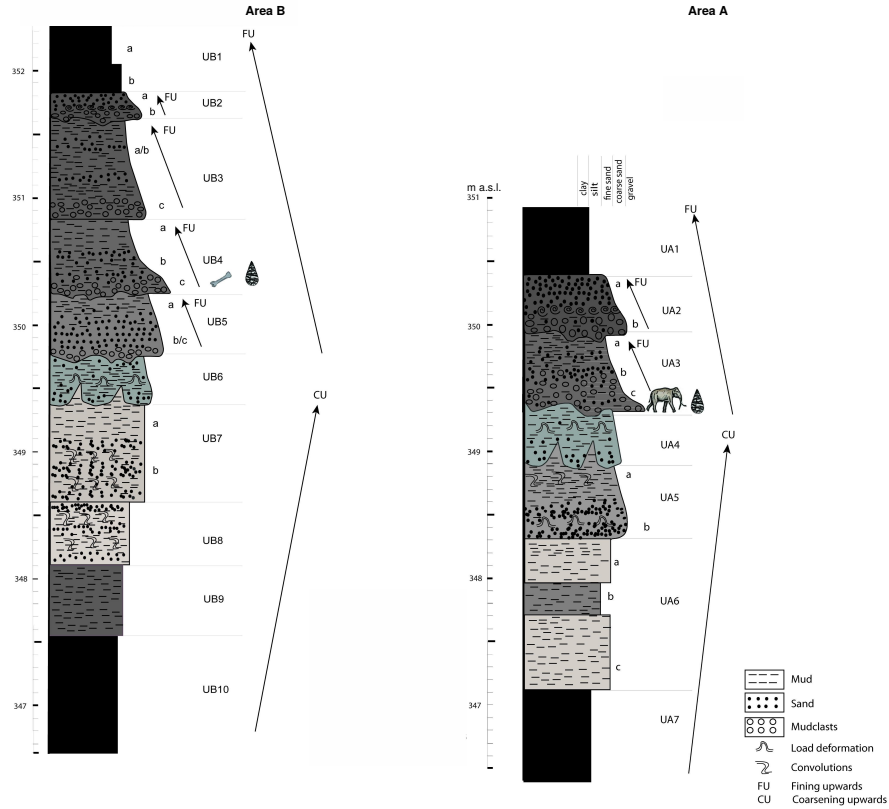


Figure 2: Stratigraphic setting of the Marathousa 1 site, modified after Karkanas et al. (this volume).

79 Evidence of butchering (cut-marks) have been identified on two of the elephant bones  
 80 from Area A, as well on elephant and other mammal bones from Area B (Konidaris et  
 81 al., this volume).

82 An erosional contact separates the two main find-bearing units in both areas, namely  
 83 UA3c/4 and UB4c/5a (Fig. 2). In Area A, the elephant remains lie at the contact of  
 84 UA3c/4 and are covered by UA3c. In Area B, most of the material were collected from  
 85 unit UB4c. For both areas, the working hypothesis is that the flow event represented by  
 86 units UA3c and UB4c eroded an exposed surface (where the elephant was lying) and  
 87 scoured this surface, thereby entraining clastic material (including probably artefacts)  
 88 and re-depositing it at close distance (see Karkanas et al., this volume).

89      The erosional event described above, and specifically the erosional contacts be-  
90      tween the fossiliferous horizons in the two areas, provide the essential background for  
91      the analysis and interpretation of the spatial distributions at Marathousa 1.

92      The secondary deposition nature of the main find horizons raises the question of  
93      how reliable is the spatial association between the lithic artefacts and the partial skele-  
94      ton of a single individual of *Elephas (Palaeoloxodon) antiquus* and the other faunal  
95      remains. Since spatial association does not necessarily imply causation, the answer has  
96      important consequences for the interpretation of the site in the broader context of the  
97      Middle Pleistocene human-proboscidean interactions. We aim to tackle this question  
98      and disentangle the formation processes acting at Marathousa 1 on the basis of spatial  
99      patterns through a three-prong spatial analytic approach:

- 100     1. by analysing, in a frame of references, the fabric of remains from relevant strati-  
101        graphic units;  
102     2. by quantifying and comparing their relative vertical distributions;  
103     3. by identifying spatial trends in either the assemblage intensities and the associa-  
104        tions between classes of remains.

105     **3. Material and methods**

106     Since 2013, systematic investigation of the Marathousa 1 site has been carried out  
107     by a joint team from the Ephoreia of Palaeoanthropology-Speleology (Greek Ministry  
108     of Culture) and the University of Tübingen. A grid of 1 square meter units was set up,  
109     oriented -14 degrees off the magnetic North, and including the two areas of investiga-  
110     tion. The excavation of the deposit proceeded into sub-squares of 50x50 cm in Area  
111     B and 1x1 m squares in Area A, and spits of about 5 to 10 cm thickness, respectively.  
112     Systematic screen-washing of sediments was carried out on-site using 1 mm sieves,  
113     in order to guarantee recovery of the small-size fraction (e.g., micro-artefacts, small  
114     mammal remains, fish, molluscs and small fragments of organic and inorganic mate-  
115     rial). The three-dimensional coordinates of finds (i.e., all the lithic artefacts, teeth and  
116     diagnostic bones; bones and organic material with a-axis  $\geq 20$  mm), collected spits  
117     of sediment, samples and geological features (e.g., erosional contacts and mud cracks)

118 were recorded with the use of a Total Station. The dimensions (length, width and thick-  
119 ness) of registered finds were measured on-site with millimetre rules. Orientation (dip  
120 and strike) of elongated particles (i.e., faunal remains, large wood fragments and lithic  
121 artefacts) was recorded since 2013 with a 30 degree accuracy, using a clock-like sys-  
122 tem (the strike was measured, relatively to the grid North, in twelve clockwise slices).  
123 In 2015, the use of a compass and inclinometer with an accuracy of 1 degrees was in-  
124 troduced in Area B to gradually replaced the former method. Strike (azimuth) and dip  
125 measurements were taken along the a-axis (symmetrical longitudinal axis) of the bones  
126 ([Domínguez-Rodrigo and García-Pérez, 2013](#)), the lithic artefacts ([Bertran and Texier,](#)  
127 [1995](#)) and organic material, using the lowest endpoint of the axis as an indicator of the  
128 vector direction.

129 The present study focuses on the excavated stratigraphic units in which most of the  
130 archaeological and palaeontological remains were recovered in both excavation areas,  
131 namely UA3c and UA4 in Area A, and UB4c and UB5a in Area B. From the total,  
132 subset samples of material were used for each specific spatial analysis. For the fabric  
133 analysis we included material collected until 2016. For the vertical distribution and  
134 point pattern analyses, the region of investigation was limited to the squares excavated  
135 from 2013 until 2015, 25 and 29 square meters respectively in each area.

136 The analyses were performed in R statistical software ([R Core Team, 2016](#)). In  
137 order to make this research reproducible ([Marwick, 2017](#)), a repository containing a  
138 compendium of data, source code and text is open licensed available at the DOI:...

### 139 *3.1. Fabric analysis*

140 Comparative fabric analysis was conducted with the aim to investigate the dynam-  
141 ics of the depositional processes at Marathousa 1. The analysis of the orientation of  
142 elongated clasts can distinguish three main types of pattern (isotropic, planar and linear  
143 fabric), each one associated with different sedimentary processes.

144 At the margin of a lacustrine environment, relatively close to the surrounding relief,  
145 a combination of high- and low-energy processes can be expected. According to the  
146 depositional context of the site (Karkanas et al., this volume), a strong preferred ori-  
147 entation of clasts (linear pattern) would suggest the action of massive slope processes

such as mudslides and debris / hyperconcentrated flows. On the other hand, whereas the frontal lobes of debris flows have been found to show a more random orientation (isotropic pattern), overland flows have been associated with planar fabrics ([Lenoble and Bertran, 2004](#)). Conversely, in a lacustrine floodplain, anisotropy without significant transport can be caused by low-energy processes such as lake transgression and regression, as well as water-sheet formed during rainy seasons. Isotropic patterns have been observed in different parts of mudflats as well ([Cobo-Sánchez et al., 2014](#)).

Nevertheless, grey zones exist between different depositional processes, so that an unequivocal discrimination based only on fabric observations is often not possible, and other taphonomic criteria must also be considered.

Since fabric strength has been found to be positively correlated with the shape and size of the clast, for the fabric analysis we subset samples of remains with length  $\geq 2$  cm and elongation index (the ratio length/width)  $I_e \geq 1.6$  ([Lenoble and Bertran, 2004](#)). The samples are listed in Table 1 and include mostly wood fragments and faunal remains from the four stratigraphic units studied here. No distinction of skeletal elements was made, both due to the high fragmentation rate of faunal remains in Area B, and because recent experiments showed a similar orientation pattern for different bone shapes ([Domínguez-Rodrigo and García-Pérez, 2013; Domínguez-Rodrigo et al., 2012](#)).

The sample of bones belonging to the individual of *Elephas (P.) antiquus* from Area A was analysed separately and included the humerus, ulna, femur and tibia; the atlas, axis and 16 complete vertebrae or vertebra fragments; 29 complete ribs or rib fragments; 2 calcanea; 4 metatarsals/metacarpals; the pyramidal; the trapezoid and the pelvis. The sample from UB5a was too small (only 7 observations) and was therefore excluded. The sample from the UB4c unit was divided in two sub-samples considered separately: those recorded using the clock method and those recorded using the compass method. All the sampled observations are representative of the whole area of interest.

Rose diagrams and uniformity tests, such as Rayleigh, Kuiper, Watson and Rao tests ([Jammalamadaka et al., 2001](#)), were used to visualise and evaluate circular isotropy in the sample distribution. The Rayleigh test is used to assess the significance of the

Table 1: List of sampled observations for the fabric analysis.

Sample	<i>n</i>	Type		
		Fauna	Wood	Lithic
UA3c	49	23	25	1
UA4	38	8	30	-
<i>E. (P.) antiquus</i>	63			
UB4c (clock)	86	68	4	14
UB4c (compass)	65	47	10	8

179 sample mean resultant length ( $\bar{R}$ ), assuming that the distribution is unimodal and not  
 180 bi- or plurimodal. The  $\bar{R}$  ranges from 0 to 1: values close to 1 indicate that the data are  
 181 closely clustered around the mean direction; when the data are evenly spread  $\bar{R}$  has a  
 182 value close to 0. A *p-value* lower than 0.05 rejects the hypothesis of randomness with  
 183 a 95% confidence interval. Kuiper, Watson and Rao are omnibus tests used to detect  
 184 multimodal departures from circular uniformity. All of them were applied using a sig-  
 185 nificance level of *alpha* = 0.01. The test results were evaluated against critical values:  
 186 a result higher than the critical value rejects the null hypothesis of isotropy with a 99%  
 187 confidence interval.

188 Randomness testing of three-dimensional data was conducted with the Woodcock  
 189  $S_1/S_3$  test (Woodcock and Naylor, 1983). Considering both the dip (plunge) and strike  
 190 (bearing) of the oriented items, this method, based on three ordered eigenvalues ( $S_1$ ,  
 191  $S_2$ ,  $S_3$ ), is able to discriminate the shape and strength of the distributions. The shape  
 192 parameter  $K = \frac{\ln(S_1/S_2)}{\ln(S_2/S_3)}$  ranges from zero (uni-axial girdles) to infinite (uni-axial clus-  
 193 ters). The parameter  $C = \ln(S_1/S_3)$  expresses the strength of the preferential ori-  
 194 entation, and its significance is evaluated against critical values from simulated random  
 195 samples of different sizes. A perfect random uniform distribution would have  $C = 0$   
 196 and  $K = 1$ .

197 The Benn (Benn, 1994) diagram adds to the Woodcock test an isotropy ( $IS =$   
 198  $S_3/S_1$ ) and an elongation ( $ES = 1 - (S_2/S_1)$ ) index. Like the former method, it is  
 199 able to differentiate between linear (cluster), planar (girdle) or isotropic distributions.  
 200 There are no published raw data from actualistic studies on depositional processes af-

fecting the orientation of bones and artefacts deposited on lacustrine floodplains (but see Morton (2004) and Cobo-Sánchez et al. (2014) as pioneer studies on this subject). However, we included in the Benn diagram references to published results from observation of fabrics in modern subaerial slope deposits (Bertran et al., 1997; Lenoble and Bertran, 2004).

Fabric analysis is a powerful tool but, as suggested by Lenoble and Bertran (2004), it is not sufficient to unequivocally discriminate processes and should therefore be integrated with the analysis of other diagnostic features.

### 3.2. Vertical distribution

We provisionally assume that a general concentration of unsorted material in the proximity of the erosional surfaces would support an autochthonous origin of the assemblages; whereas a poorly to extremely poorly sorted and homogeneous vertical distribution of remains from the UA3c and UB4c units would suggest an allochthonous origin and a subsequent secondary deposition triggered by a massive process, e.g., debris or hyperconcentrated flows. Graded bedding could result in such fluid depositional environments, associated with a decrease in transport energy.

In order to estimate the degree of vertical dispersion while controlling for the size of the archaeological material, dimensional classes were set up following typological criteria. Lithic artefacts were classified as debris/chip when smaller than a cutoff length of 15 mm (see Tourloukis et al., this volume). Other classes include flakes, tools and cores; the latter being the bigger and heavier debitage product. Table 2 summarises the sample size for each class. Lithic debris/chips constitutes the larger part of the assemblages from UB4c (60%) and UB5a (49%); whereas in Area A it represents only a moderate percentage in the upper UA3c unit (16%). The very rare presence of lithic artefacts in the underlying unit UA4 is nevertheless significant. In this unit, the faunal remains are also found in much lower numbers, their number reduced to one fourth of those found in UA3c. For the point pattern analysis (see below), we used the same subset of materials for both excavation areas.

For Area B, the material recovered from the water-screening was randomly provenanced according to the 5 cm depth of the excavated spit and the coordinates of the

Table 2: List of sampled observations for the vertical distribution and point pattern analyses.

Sample	<i>n</i>	Lithic class					Faunal class			
		Debris/chip	Flake	Bone flake	Tool	Core	Indet.	Bone	Tooth	Microfauna
UA3c	279	46	2	-	1	-	1	171	14	44
UA4	61	3	1	-	-	-	-	45	4	8
UB4c	1243	753	154	1	34	6	2	246	28	19
UB5a	101	50	12	-	3	-	-	30	3	3

50x50 cm quadrant of the excavation square. Following the same excavation protocol, the same procedure was applied for the water-screened material of Area A, which was randomly provenanced according to 3D-coordinates of the 1x1 m excavation square and 10 cm spit.

Inverse-distance weighting (IDW) interpolation of the recorded points of contact between the UB4c/5a and UA3c/4 stratigraphic units were used to reconstruct their erosional surfaces, in Areas A and B, respectively (Fig. 3a,b). IDW assumes spatial autocorrelation and calculates, from a set of irregular known points, weighted average values of unknown points. Thus, in order to address our specific objective, i.e., to quantify and analyse the vertical distribution of the archaeological and palaeontological material, we measured the minimum orthogonal distance of each specimen to the interpolated erosional surface (Fig. 3c).

For the units above and below this surface (i.e., UB4c and UB5a), the relative distribution of lithic classes and faunal remains was informally tested by means of kernel density estimations. Likewise, in Area A the relative vertical distribution of remains from UA3c was estimated relative to the absolute elevation of the elephant remains and the range of elevations of the UA3c/4 surface. Finally, a Student's two sample t-test allowed us to compare the empirical distributions of different groups of remains for each stratigraphic unit.

### 3.3. Point pattern analysis

A spatial point pattern is defined as the outcome of a random spatial point process (repetitions of it would always create a different pattern). The observed patterns of the archaeological and palaeontological remains were treated as manifestations of spatial

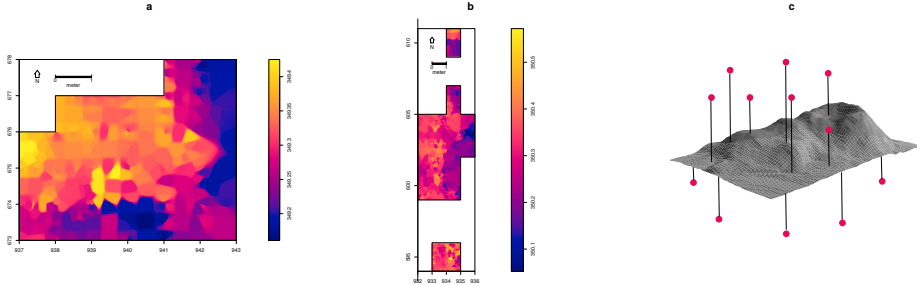


Figure 3: IDW interpolation of the UA3c/4 (a) and UB4c/5a (b) points of erosional contact; the color scale denotes elevation a.s.l. Illustration of the method used to quantify the vertical dispersion of remains with respect to the UB4c/5a surface (c).

254 point processes, i.e., site formation processes. Point pattern analysis investigates the  
 255 spatial arrangement of points with the aim to identify spatial trends. In order to integrate  
 256 the previous studies of the fabric and vertical distributions, we directed our point  
 257 pattern analysis equally to the intensity of the patterns (the rate of occurrence of the  
 258 recorded finds) and to the spatial interaction between different types of finds.

259 As the average number of random points per unit area, intensity informs about homogeneity or inhomogeneity in the distribution of events generated by a point process,  
 260 i.e., whether the rate of occurrence is uniform or spatially varying across the study area.  
 261 Intensity, usually non-parametrically evaluated by means of kernel density estimation  
 262 ([Diggle, 1985](#)), was assessed for the distribution of material from the UB4c, UB5a  
 263 and UA3c units. Cross-validation bandwidth, which assumes a Cox process, and edge  
 264 correction were applied using the methods described in [Diggle \(1985\)](#).

266 In the presence of a covariate, it is recommended to further investigate the dependence  
 267 of intensity on that explanatory variable. In order to evaluate whether variation  
 268 in the density of materials was correlated to the topography of the erosional surface,  
 269 we computed a local likelihood smoothing estimate of the intensity of remains from  
 270 UB4c as a function of the UB4c/5a surface elevation model ([Baddeley et al., 2012](#)).  
 271 Formal tests enabled us to assess the evidence of that dependence and to quantify the  
 272 strength of the covariate. The Kolmogorov-Smirnov test of CSR (Complete Spatial  
 273 Randomness) and Berman's  $Z_2$  statistics were used to test the strength of evidence for

274 a covariate effect. The Receiver Operating Characteristic (ROC) plot, and the area  
275 under the ROC curve (AUC), closely related to Berman's  $Z_2$  test, measure the magni-  
276 tude of the covariate effect. AUC values close to 1 or 0 indicate strong discrimination,  
277 whereas intermediate values (0.5) suggest no discrimination power.

278 Whereas intensity is a first-order property of the point process, multiscale inter-  
279 point interaction is measured by second or higher-order moment quantities, such as  
280 the Ripley's  $K$  correlation function (Ripley, 1976, 1977) and the distance  $G$ -,  $F$ - and  
281  $J$ -functions. Three different types of inter-point interaction are possible: random, reg-  
282 ular or cluster. Regular patterns are assumed to be the result of inhibition processes,  
283 while cluster patterns are the result of attraction processes. In order to reduce the  
284 edge effect bias in estimating the correlation between points, we implemented Rip-  
285 ley's isotropic edge correction (Ohser, 1983; Ripley, 1988). In a hypothesis-testing  
286 framework, pointwise envelopes were computed by 199 random simulations of the  
287 null hypothesis. Thus, values of the empirical distribution (black solid line) were plot-  
288 ted against the benchmark value (red dotted line) and the envelopes (grey area) which  
289 specify the critical points for a Monte Carlo test (Ripley, 1981).

290 In order to test the spatial dependence between remains associated with the ero-  
291 sional event of UB4c and those associated with the underlying UB5a unit, we treated  
292 the data as a multivariate point pattern, assuming that the point patterns in UB4c and  
293 UB5a are expressions of two different stationary point processes, i.e., depositional  
294 events. We performed a cross-type pair correlation function ( $g_{ij}(r)$ ), derivative of the  
295 multitype  $K_{ij}(r)$  function, which is the expected number of points of type  $j$  lying at a  
296 distance  $r$  of a typical point of type  $i$ . The function is a multiscale measurement of the  
297 spatial dependence between types  $i$  (UB4c) and  $j$  (UB5a). Randomly shifting each of  
298 the two patterns, independently of each other, estimated values of  $\hat{g}_{ij}(r)$  are compared  
299 to a benchmark value  $g_{ij}(r) = 1$ , which is consistent with independence or at least with  
300 lack of correlation between the two point processes.

301 In addition to the pair correlation function, the multitype nearest-neighbour  $G_{ij}(r)$   
302 function was used to estimate the cumulative distribution of the distance from a point of  
303 type  $i$  (UB4c) to the nearest point of type  $j$  (UB5a). It measures the spatial association  
304 between the two assemblages. For the cross-type  $G$ -function, the null hypothesis states

305 that the points of type  $j$  follow a Poisson (random) distribution in addition to being  
306 independent of the points of type  $i$ . Thus, in a randomisation technique, when the solid  
307 line of the observed distribution ( $\hat{G}_{ij}(r)$ ) is above or below the shaded grey area, the  
308 pattern is significantly consistent with clustering or segregation, respectively. Complete  
309 spatial randomness and independence (CSRI) of the two point processes would support  
310 an exogenous origin hypothesis for the assemblage recovered from the UB4c unit. On  
311 the other hand, positive or negative association can be interpreted as expression of  
312 different endogenous processes.

313 The particle size spatial distribution of the lithic assemblage from UB4c was inves-  
314 tigated by means of a transformation of the multitype  $K$ -function ( $K_{i\bullet}(r) - K(r)$ , see  
315 [Baddeley et al. \(2015\)](#), p.608). In this case, we treated the data as the manifestation of a  
316 single multitype point process. In a joint distribution analysis, the locations and types  
317 of points are assumed to be generated at the same time. The null model of a random  
318 labelling test states that the type of each point is determined at random, independently  
319 of other points, with fixed probabilities. The estimated  $K$ -function for a subset of pos-  
320 sible combinations was evaluated against the envelope of Monte Carlo permutations of  
321 the class of remains. Likewise with the vertical distribution, a horizontal clustering of  
322 small specimens, such as lithic debris/chips, together with larger dimensional classes  
323 of remains would suggest the lack of sorting by natural depositional processes and a *en*  
324 *mass* model of deposition.

325 As for the three-dimensional distribution of the lithic artefacts in Area A, and their  
326 spatial association with the partial skeleton of the *E. (P.) antiquus*, we applied three-  
327 dimensional univariate and bivariate second-order functions. A rectangular box of 20  
328 square meters and 80 cm vertical extent was selected for the analyses (green outline in  
329 Fig. 9a). Assuming homogeneity, the univariate pair correlation function ( $g_3(r)$ ) was  
330 estimated for the pattern of all the artefacts (mostly debris/chips) from UA3c and UA4.  
331 In the specific context of the site, complete spatial randomness (CSR) would suggest  
332 that the pattern most probably is the result of a random distribution process, such as  
333 a high energy mass movement. In contrast, other natural processes would produce  
334 clustering or segregation of the lithic artefacts. Spatial aggregation, if not generated by  
335 obstructions, would support an *in situ* primary origin of the assemblage.

Table 3: Global tests for circular uniformity

Sample	mean dir.	Rayleigh		Kuiper		Watson		Rao		level
		$\bar{R}$	p - value	test	critical value	test	critical value	test	critical value	
UA3c	77.17°	0.268	0.029	2.4698	2.001	0.2967	0.267	271.8367	160.53	0.01
UA4	35.79°	0.386	0.003	2.5656	2.001	0.3437	0.267	246.3158	163.73	0.01
<i>E. (P.) antiquus</i>	54.64°	0.489	2.775e-07	3.4811	2.001	0.906	0.267	291.4286	155.49	0.01
UB4c (clock)	83.96°	0.167	0.091	2.327	2.001	0.2466	0.267	309.7674	155.49	0.01
UB4c (compass)	128.14°	0.225	0.037	1.6917	2.001	0.1862	0.267	153.3846	155.49	0.01

336 In support to the pair correlation function, the cross-type nearest-neighbour func-  
 337 tion has been applied in order to compute, for each artefact recovered from the UA3c  
 338 and UA4 units, the nearest point associated with the elephant skeleton. A prevalence  
 339 of short distances would indicate aggregation of the lithic artefacts around the mass  
 340 of the elephant; whereas a uniform or symmetric distribution would support random  
 341 independent processes.

## 342 4. Results

### 343 4.1. Fabric analysis

344 The rose diagrams in Fig. 4 visualise the circular distributions of the examined  
 345 specimens. Overall, the UA4 sample and the sample of elephant bones show predomi-  
 346 nant peaks in the NE quadrant; while the ones from units UA3c and UB4c suggest uni-  
 347 form to multimodal distributions. Specifically, the UA4 sample distribution (Fig. 4b)  
 348 spreads largely in the NE quadrant. Similarly, the circular distribution of the elephant  
 349 sample (Fig. 4c), mainly lying in UA4, resembles the former distribution: it is skewed  
 350 to the SW and concentrated in the NE quadrant. On the other hand, the UA3c sample  
 351 (Fig. 4a) and the two samples from Area B (Fig. 4d,e) suggest a different isotropic  
 352 scenario.

353 Table 3 summarises the results of the circular uniformity tests. With regard to the  
 354 UA3c sample, the Rayleigh test ( $p - \text{value} = 0.029$ ) rejected the null hypothesis of  
 355 circular uniformity. The mean resultant length ( $\bar{R} = 0.268$ ) and the mean direction  
 356 of 77.17° are thus significant, assuming the distribution is unimodal. However, the  
 357 Kuiper, Watson and Rao omnibus tests also rejected the null hypothesis of uniformity,

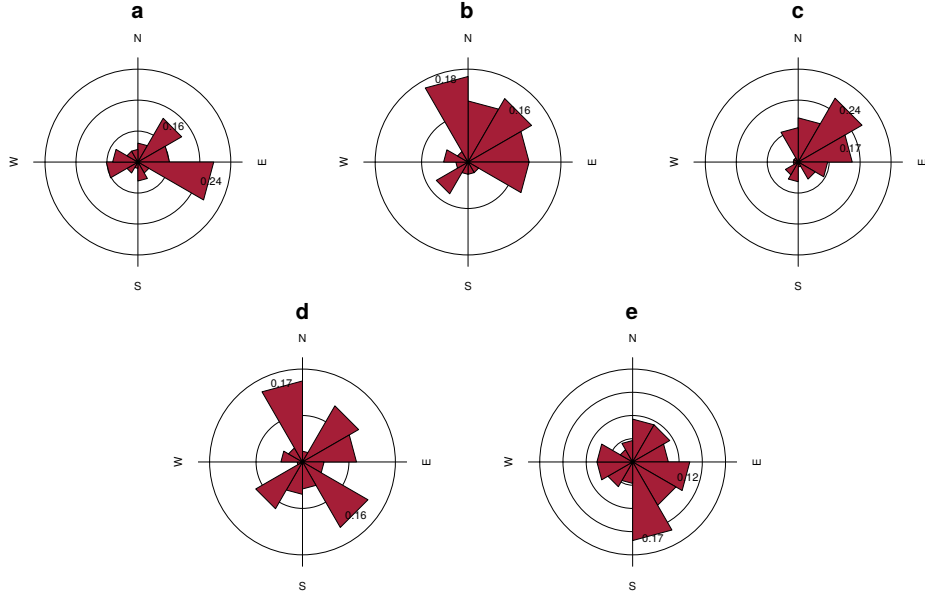


Figure 4: Rose diagrams showing the bearing patterns of samples from UA3c (a), UA4 (b), the elephant carcass (c) and UB4c (d: clock method, e: compass method)

358 therefore suggesting multimodal anisotropy in the distribution, as shown by the rose  
 359 diagram (Fig. 4a).

360 For the UA4 sample and the subset of elephant bones, all the tests agreed in rejecting  
 361 the null hypothesis in favour of a preferentially oriented distribution. The Elephant  
 362 sample, with respect to the other, showed stronger anisotropy and significantly higher  
 363  $\bar{R}$ . As suggested by the rose diagrams (Fig. 4c), this sample has a mean direction to-  
 364 wards the NE ( $55^\circ$ ) and relatively low circular variance ( $29^\circ$ ).

365 The UB4c sub-samples had discordant test results when considering the Rayleigh  
 366 and the omnibus statistics. According to the Rayleigh test, the mean resultant length  
 367 ( $\bar{R}$ ) and the mean direction were not significant for the sub-sample of measurements  
 368 recorded with the clock system. Conversely, a weak significant test result was obtained  
 369 for the sub-sample of measurements recorded using the compass. Overall, for the latter  
 370 sub-sample all the omnibus tests suggested significant isotropy (Fig. 4e). On the other  
 371 hand, the Kuiper and Rao tests, suggested a multimodal departure from uniformity for  
 372 the sample recorded using the clock method (Fig. 4d).

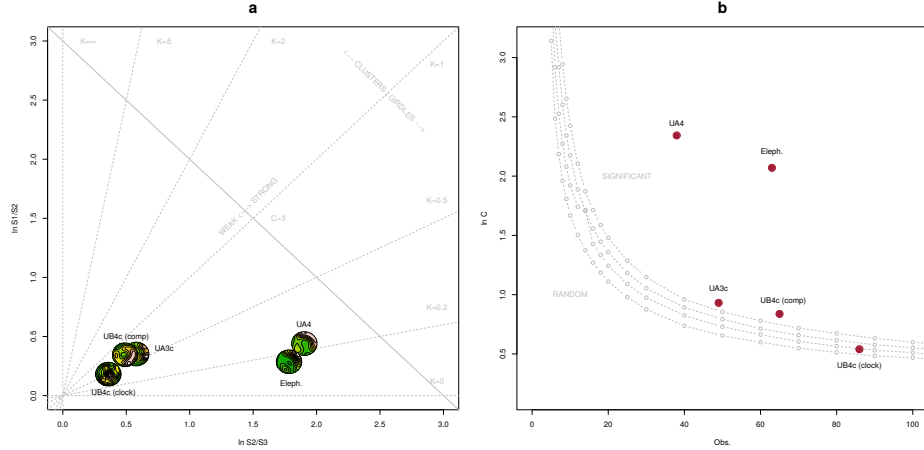


Figure 5: Woodcock's eigenvalues ratio graph (a) and plot of the Monte-Carlo critical  $S_1/S_3$  test values, for varying sample sizes and confidence levels (b), modified from [Woodcock and Naylor \(1983\)](#).

373     The results obtained for the UA3c sample and the UB4c sub-sample recorded using  
 374     the clock method are most probably due to the shape of those distributions. Indeed, the  
 375     clock system, being less accurate, tends to produce a less dense distribution, more  
 376     subject to show a multimodal shape when the distribution is actually uniform (Fig. 4a,  
 377     d).

378     The Woodcock eigenvalues ratio graph (Fig. 5a) presents the shape ( $K$ ) and strength  
 379     ( $C$ ) of the distributions. Fig. 5b plots confidence levels of Monte-Carlo critical  $C$  val-  
 380     ues, varying for sample sizes. The two samples from Area B, together with the UA3c  
 381     sample, having low  $C$  values, plotted close to the origin of the ratio graph. Thus, they  
 382     suggest nearly significant randomness. On the other hand, the UA4 and the elephant  
 383     samples, with higher  $C$  values, showed a stronger and significant tendency to orient  
 384     preferentially. The shape parameter  $K$  of the samples varied from  $K = 0.7$  for the  
 385     UB4c sample measured with the compass to  $K = 0.1$  for the elephant sample. Overall,  
 386     all the samples plotted below the average shape value ( $K = 1$ ) between girdles and  
 387     clusters distributions.

388     The Benn diagram (Fig. 6) resembles the Woodcock ratio graph (Fig. 5a). The  
 389     samples from units UB4c and UA3c clearly plotted at a distance from the UA4 and the  
 390     elephant samples. The UB4c sub-sample of measurements recorded with the compass,

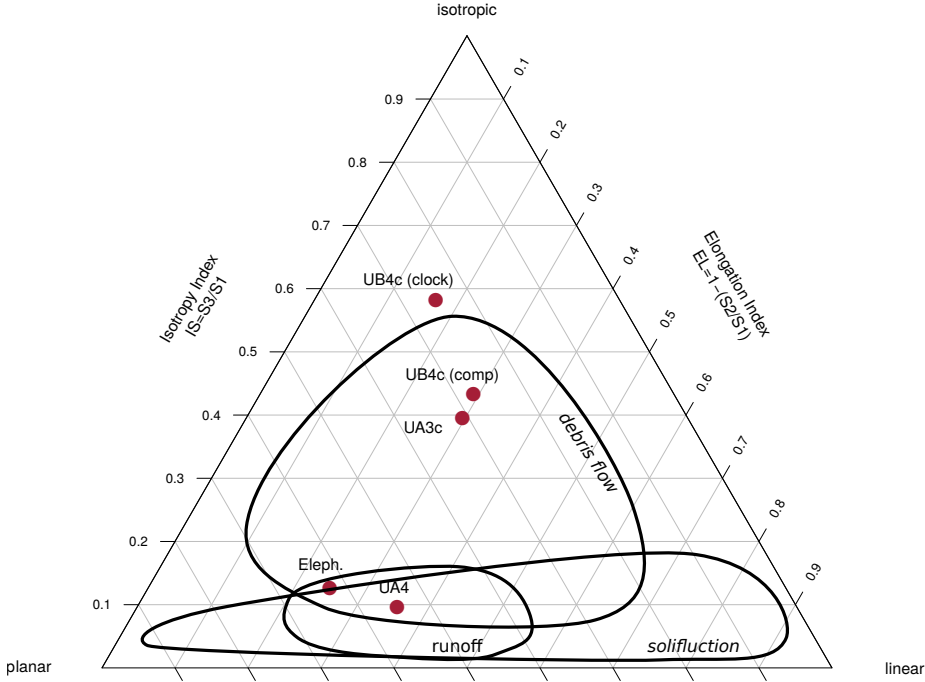


Figure 6: Benn's diagram. Fabric ranges of natural processes modified from Bertran et al. (1997); Lenoble and Bertran (2004).

391 together with the UA3c sample, plotted in the centre of the ternary graph. As shown  
 392 above, the UB4c sub-sample of measurements taken using the clock system exhibited  
 393 more isotropy.

394 Compared to the ranges recorded for modern natural processes (debris flow, runoff,  
 395 solifluction), the fabric from the UA3c and UB4c units plotted well inside the cluster of  
 396 debris flows, with the UB4c (clock) sample suggesting even more random orientations.  
 397 On the other hand, the sample of elephant remains, which lie mostly on UA4 and are  
 398 covered by UA3c, plotted significantly close to the sample from unit UA4. They both  
 399 presented the lowest isotropy index ( $IS$ ), but not high elongation index ( $EL$ ). Thus,  
 400 they plotted in the average between linear and planar orientations, within the range of  
 401 runoff processes. Yet they still plotted at the margins of the cluster of debris flows  
 402 fabrics. Moreover, the elephant sample showed a more planar attitude with respect to  
 403 the UA4 sample.

404     4.2. Vertical distribution

405     Fig. 7 compares the distribution of the absolute elevations of the partial skeleton of  
406     the *Elephas (P.) antiquus* with the other remains from Area A. Overall, the vertical dis-  
407     tribution of the elephant approximates a normal distribution with mean ( $\mu$ ) 349.25 m  
408     a.s.l. and standard deviation ( $\sigma$ ) 0.12 m. The mean elevation of the erosional con-  
409     tact between the two stratigraphic units is slightly above the latter ( $\mu = 349.30$  m).  
410     Although difficult to quantify due to its not sharp nature, the range of elevations of  
411     this contact, as estimated from the IDW interpolation (Fig. 3a), is relatively small  
412     ( $\sigma = 0.06$  m).

413     Three lithic artefacts (two flakes and one tool) from the UA3c unit are located  
414     within its positive half. Only one flake has been found in the lower UA4, at about  
415     349.10 m, together with three chips. However, they plotted well within the left tail  
416     of the debris/chip distribution from the unit above. Despite the scarcity of debitage  
417     products in this area, waste products (debris/chip) are relatively well represented (16%  
418     of the UA3c sample). Their vertical distribution approximates a normal distribution  
419     ( $\mu = 349.50$  m and  $\sigma = 0.18$  m), having almost 50% of the sample in the range of  
420     elevations of the erosional surface and the rest above it. Notably, the distribution of  
421     the faunal remains from the same unit resembles that of the debris/chip. The Welch  
422     two sample t-test ( $p - value = 0.5099$ ) failed to reject the null hypothesis that the  
423     two population means are equal. On the other hand, the vertical distribution of faunal  
424     remains recovered from the UA4 unit is comparable with that of the *Elephas* ( $p -$   
425      $value = 0.6562$ ). Nevertheless, the density functions altogether clearly confirm one  
426     of the main observations assessed during excavation, namely that the elephant remains  
427     and most of the recovered faunal and lithic material in Area A lie at or close to the  
428     UA3c/4 contact, with unit UA3c covering the remains.

429     Fig. 8 shows the empirical density functions of the minimum distances from each  
430     specimen from Area B to the UB4c/5a erosional contact (Fig. 3b). The combined  
431     distribution of any type of find from the UB5a unit (Fig. 8a) skewed to the left with  
432     a short tail (up to -0.3 m). The mode, between 5 and 10 cm below the roof of UB5a,  
433     indicates a general concentration of material very close to the contact of this unit with  
434     the overlying UB4c, in accordance with the mean distribution of the different classes of

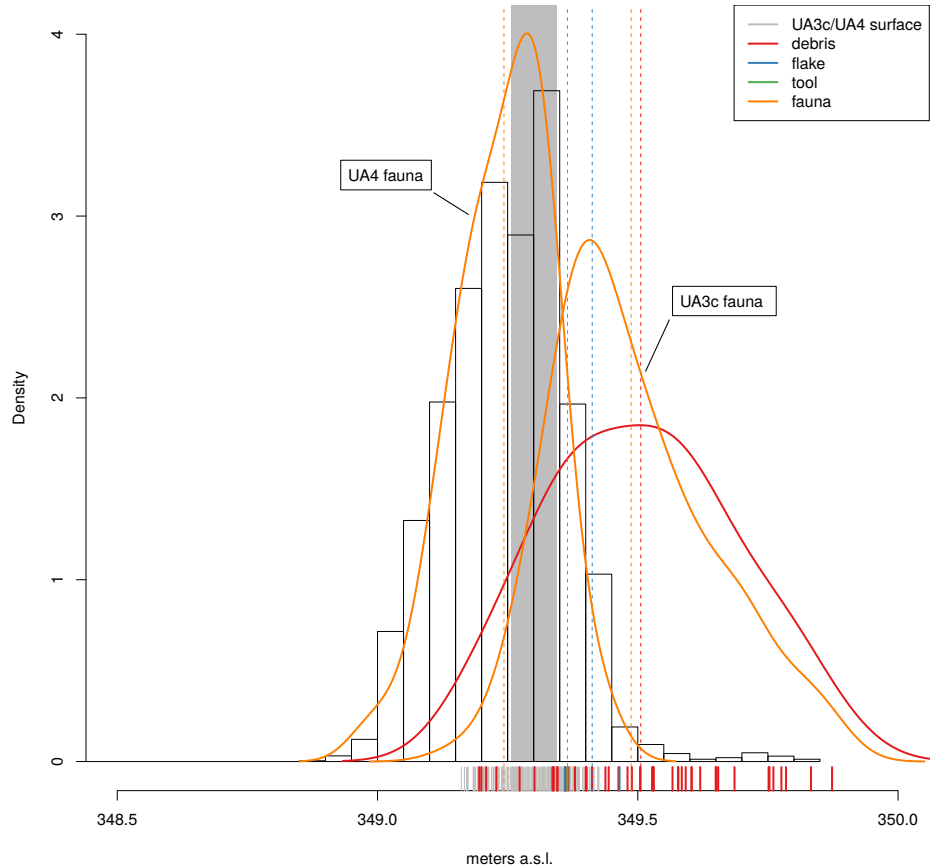


Figure 7: Empirical density functions of absolute elevations (meters a.s.l) of remains from Area A. The histogram represents the *Elephas (P.) antiquus* range of elevations; the grey area shades the  $Q_3 - Q_1$  range of the erosional UA3c/4 surface; dashed lines indicate mean values.

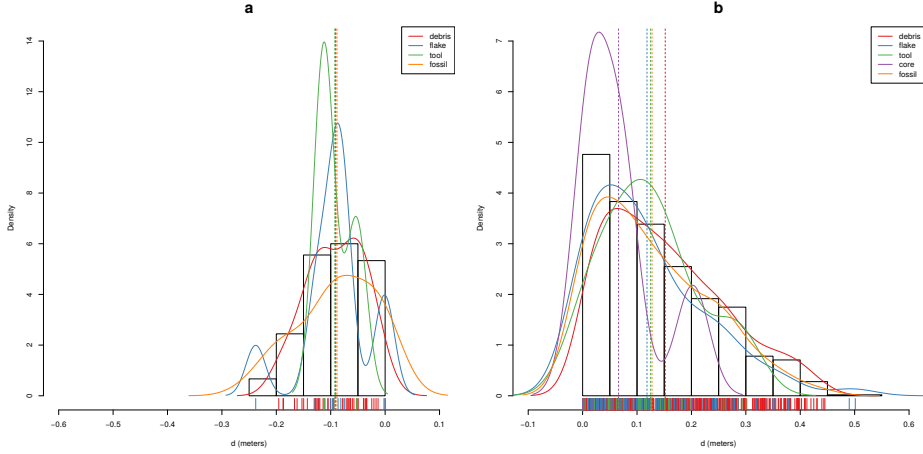


Figure 8: Empirical density functions of minimum orthogonal distances ( $d$ ) to the UB4c/5a surface. The histogram represents the total distribution of remains from UB5a (a) and UB4c (b); dashed lines indicate mean values.

435 remains. Although the majority of both the lithic and faunal assemblages were found  
 436 in the uppermost 15 cm of UB5a, few debris/chips and bone fragments occur lower  
 437 in the sequence, yet no more than 30 cm below the roof of this unit. Very few flakes,  
 438 three tools and no cores have been found in this unit. As a whole, the lithic assemblage  
 439 from UB5a, mostly composed by debris/chips, is only 7% of the most conspicuous  
 440 assemblage from UB4c.

441 The global distribution of unit UB4c was right skewed (up to almost 0.6 m) and cen-  
 442 tered at about 5 cm above the contact with the underlying unit UB5a (Fig. 8b). Almost  
 443 30% of the sample fell exactly at the erosional contact that separates UB4c from UB5a.  
 444 The density estimations of the lithic debris/chip, flakes, tools and faunal remains sig-  
 445 nificantly overlap, whereas the distribution of the six cores shows a bimodal shape with  
 446 peaks at 5 and 20 cm above the contact. However, the Welch Two Sample t-test of the  
 447 lithic and faunal sample means failed to reject the null hypothesis ( $p-value = 0.6295$ ).

448 *4.3. Point pattern analysis*

449 Results of the point pattern analysis are complementary to those obtained from the  
 450 analysis of the vertical and fabric distributions.

451     Regarding Area A, kernel density estimation and three-dimensional functions were  
452     applied in order to quantitatively depict the spatial distribution of the lithic assemblage  
453     in relation to the elephant skeleton.

454     Fig. 9a shows the smoothing kernel intensity estimation of the combined lithic and  
455     faunal assemblage from the UA3c unit. Contour lines delimit the density of the lithic  
456     sample. The partial skeleton of the *E. (P.) antiquus* is superimposed on it. A pre-  
457     liminary visual examination of the plot suggests a homogeneous distribution of lithics  
458     (mostly debris/chips) and fossils. Spots of higher density appear to be spread around  
459     and in association with the elephant remains.

460     The univariate pair correlation function of the joined lithic assemblage from the  
461     UA3c and UA4 units (Fig. 9b) suggests aggregation of finds. The estimated  $\hat{g}_3(r)$   
462     function (black solid line) wanders above the benchmark value (red dotted line) until  
463     values of  $r = 0.8$ . However, for distances between 35 and 65 cm, it lies above the  
464     grey envelope of significance for the null hypothesis of CSR, indicating that at those  
465     distances artefacts occur closer than expected in the case of random processes. For  
466     values of  $r > 0.8$ , the function stabilises at values close to 0, suggesting a Poisson  
467     distribution. The plot illustrates the random distribution of finds between patches of  
468     clusters that we observe in the kernel density estimation (Fig. 9a).

469     The histogram in Fig. 9c shows the density of the distances calculated from each  
470     artefact to the nearest-neighbour elephant remain. A right skewed distribution, with  
471     a prevalent peak at 10 cm and mean  $\mu \approx 30$  cm is an indication of the relatively strong  
472     aggregation of events around the mass of the elephant skeleton.

473     As for Area B, the analysis first focused on the spatial distribution and cross-  
474     correlation of the assemblages from UB4c and UB5a (Fig. 10); and secondly on the  
475     interaction between classes of remains from UB4c (Fig. 11).

476     Figs. 10a,b respectively show kernel density estimations of the combined lithic and  
477     faunal assemblages from both the units analysed. Despite the samples size difference,  
478     a first visual examination suggests the presence of interesting spatial structures.

479     Regarding the UB4c unit (Fig. 10a), the high density of material concentrated  
480     around the western square 934/600 suggests that the pattern could have been the re-  
481     sult of an inhomogeneous, non-uniform depositional process. Visual comparison of

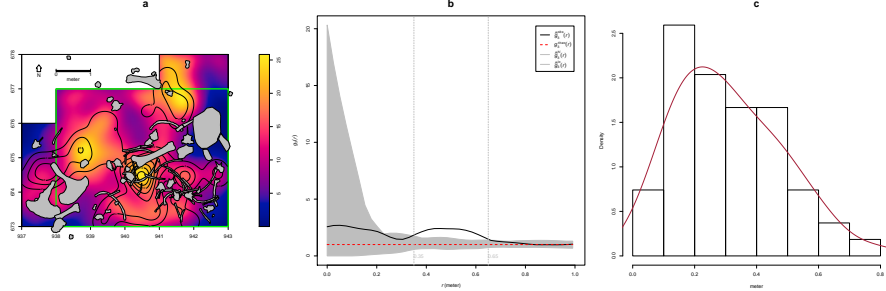


Figure 9: Kernel smoothed intensity function of the lithic and faunal assemblages from UA3c. Isolines mark the density of the lithic artefacts (a). Pair correlation function ( $g_3(r)$ ) of a three-dimensional pattern of lithic artefacts from UA3c and UA4. Grey envelope of 999 Monte Carlo simulations under the CSR null hypothesis (b). Three-dimensional distance from each lithic artefact from UA3c and UA4 to the nearest neighbour elephant remain (c).

the density plot with the elevation model of the erosional contact between the UB4c and UB5a units (Fig. 3b) suggests positive correlation between lower elevations (topographic depressions) and higher density of remains. Fig. 10c shows the results of the  $\rho$ -function, which estimates the intensity of the UB4c sample assemblage as a function of the covariate underlying topography created by the erosional event. Within the range of elevation between 350.2 and 350.4 m, the occurrence of finds is higher and the intensity decreases with the rise of elevation, i.e., finds are more likely to be found at lower elevations than would be expected if the intensity was constant.

Spatial Kolmogorov-Smirnov and Berman's  $Z_2$  (Berman, 1986) statistics were used in order to test the dependence of the UB4c pattern on the covariate erosional surface. Both KS ( $D = 0.11952$ ,  $p - value = 7.772e - 16$ ) and  $Z_2$  ( $Z_2 = -7.8447$ ,  $p - value = 4.34e - 15$ ) significantly rejected the null hypothesis of CSR. Although the tests suggested evidence that the intensity depends on the covariate, the effect of the covariate is weak and it seems to have no discriminatory power. The ROC curve and AUC statistics (0.56), which measure the strength of the covariate effect, suggest that the underlying UB4c/5a topography does not completely explain the localised high density of occurrence in the UB4c.

Relative spatial segregation seems to occur between the assemblages from UB4c

500 (Fig. 10a) and UB5a (Fig. 10b), with high density of the former distribution corre-  
501 sponding to low density of the latter. The former analysis of the vertical distribution  
502 showed that the two assemblages occur very close to their stratigraphic contact. In  
503 order to further investigate the spatial interaction between the two depositional events,  
504 we applied multitype pair correlation ( $g_{ij}(r)$ ) and nearest-neighbour ( $G_{ij}(r)$ ) functions.

505 Fig. 10d shows the estimated values of the multivariate  $\hat{g}_{ij}(r)$  function against the  
506 envelope of the null hypothesis, obtained by randomly shifting the position of remains  
507 from the two distributions in 199 Monte Carlo simulations. For fixed values of  $r$  less  
508 than 30 cm the observed function lies below the benchmark value of independence, thus  
509 indicating segregation; but it wanders at the lower edge of the grey envelope. For fixed  
510 distances of  $r > 0.3$  m the observed and theoretical lines significantly overlap. Overall,  
511 the function suggests independence of the two point processes (UB4c and UB5a) at  
512 multiple scales.

513 However, the estimated  $\hat{G}_{ij}(r)$  function (Fig. 10c), running well below the signifi-  
514 cance grey envelope for fixed values of  $r > 0.3$  m, confirms that the nearest-neighbour  
515 distances between remains from UB4c and UB5a are significantly longer than expected  
516 in the case of independent processes. Interestingly, at values of  $r < 0.2$  m the observed  
517 function failed to reject the null hypothesis of Complete Spatial Randomness and In-  
518 dependence (CSRI).

519 With the aim to integrate the vertical distribution analysis, the particle size spatial  
520 distribution of remains from the UB4c unit were investigated by means of a deriva-  
521 tive of the multitype  $K$ -function, randomly labelling the classes of remains. Fig.11  
522 shows a selection of the array of possible combinations between classes. In any panel,  
523 the estimated function wanders above the benchmark value. Such positive deviations  
524 from the null hypotheses suggest that debris/chips are more likely to be found close  
525 to the other class of remains than would be expected in case of a completely random  
526 distribution. Permutating the lithic debris/chips with flakes (Fig.11a), tools (Fig.11b),  
527 cores (Fig.11c) and faunal remains (Fig.11d), the Monte Carlo test results would have  
528 been significantly consistent with clustering, if we had chosen distance values  $r > 0.4$ ,  
529  $r > 0.4$ ,  $r > 0.9$ ,  $r > 0.8$ , respectively. Conversely, we could not reject the null  
530 hypothesis of CSRI for lesser values of  $r$ .

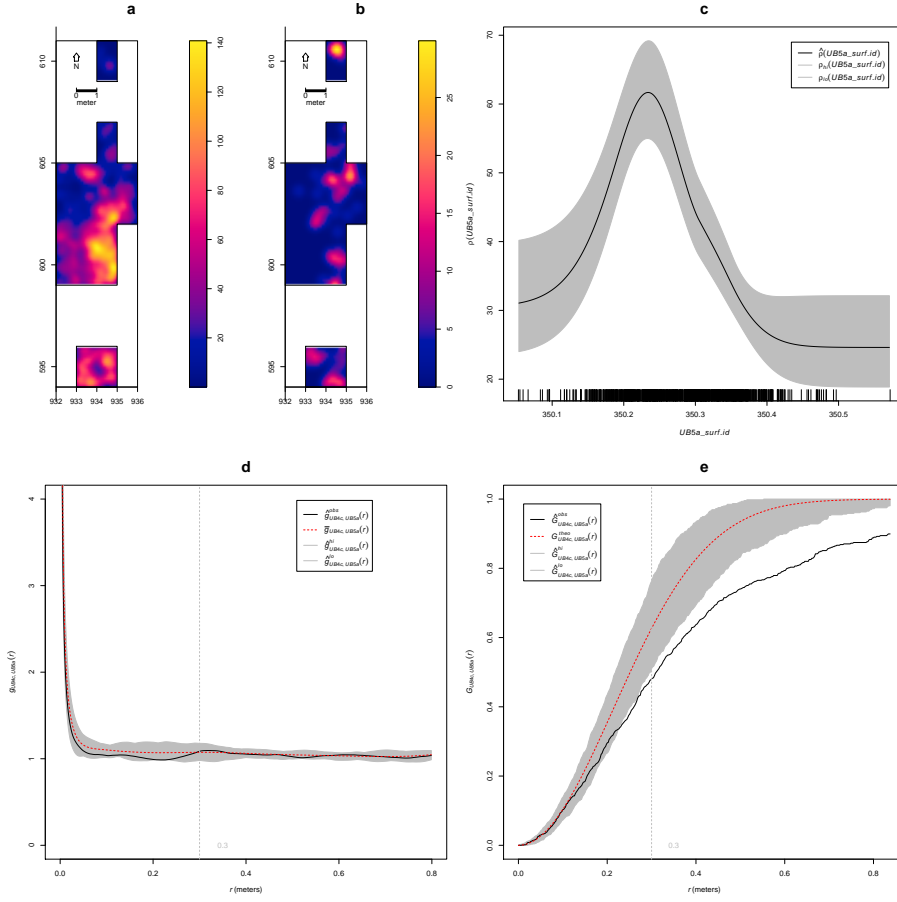


Figure 10: Kernel smoothed intensity function of the lithic and faunal assemblages from UB4c (a) and UB5a (b). Smoothing estimate of the intensity of remains from UB4c, as a function of the erosional surface UB4c/5a. Grey shading is pointwise 95% confidence bands (c). Cross-pattern pair correlation function ( $g_{ij}(r)$ ) between the UB4c and UB5a distributions. Grey envelope of 199 Monte Carlo simulations under the independence of components null hypothesis (d). Multitype nearest-neighbour function ( $G_{ij}(r)$ ) between the UB4c and UB5a distributions (e).

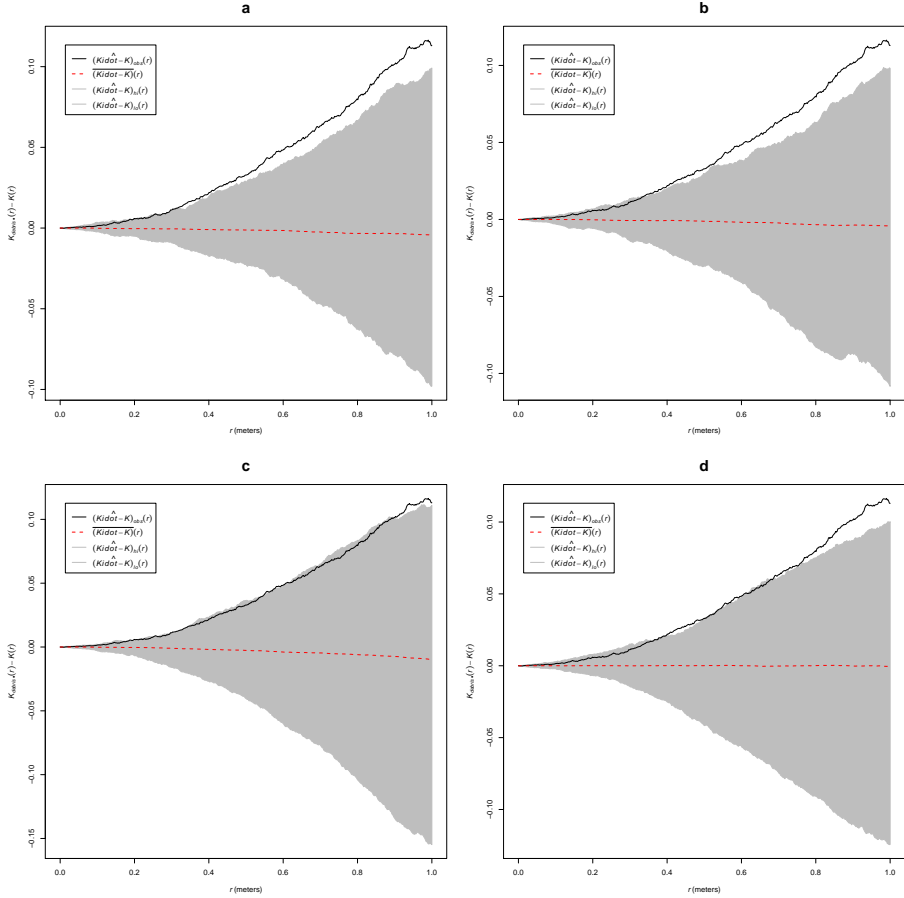


Figure 11: Random labelling test for the UB4c assemblage. Grey pointwise envelope of 199 Monte Carlo permutation of debris/chips with flakes (a); tools (b); cores (c); fossils (d).

531     **5. Discussion**

532     Recent excavations at the Middle Pleistocene site of Marathousa 1 have unearthed  
533     in one of the two investigated areas (Area A) a partial skeleton of a single individual of  
534     *Elephas (P.) antiquus*, whose bones are in close anatomical association, and spatially  
535     and stratigraphically associated with lithic artefacts and other faunal remains. In Area  
536     B, about 60 m to the South of Area A, we collected a much higher number of lithic  
537     artefacts (Tourloukis et al., this volume), spatially and stratigraphically associated with  
538     other faunal remains, including isolated elephant bones, cervids and carnivores among  
539     others (Konidaris et al., this volume).

540     The two areas are stratigraphically correlated, the main fossiliferous layers (UA3c  
541     and UB4c) representing a relatively low-energy depositional process, such as a hyper-  
542     concentrated flow that dumped material in a lake margin context (Karkanas et al., this  
543     volume).

544     To date, evidence of butchering (cut-marks) has been identified on two bones of  
545     the elephant skeleton from Area A, as well on elephant and other mammal bones from  
546     Area B (see Konidaris, this volume).

547     However, due to the secondary deposition nature of the main fossiliferous hori-  
548     zon, it is of primary importance to evaluate the degree and reliability of the spatial  
549     association of the lithic artefacts with the faunal remains, and especially with the ele-  
550     phant skeleton. In order to tackle our main objective, we applied a comprehensive  
551     set of spatial statistics to the distributions of the archaeological and zooarchaeologi-  
552     cal/palaeontological remains from relevant stratigraphic units of the two areas of in-  
553     vestigation. Preliminary results are here discussed for both areas.

554     **5.1. Fabric analysis**

555     The analysis of the orientation (dip and strike) of subsets of remains, mostly bone  
556     fragments, organic residues and lithic artefacts, showed different patterns for the two  
557     main find-bearing units.

558     The test results (Tab. 3) for the UA4 sample and the sample of elephant remains  
559     - which lie on unit UA4 and are covered by UA3c - indicated significant preferential

560 orientations towards the NE (Figs. 4b,c). As shown by the Woodcock's (Fig. 5) and the  
561 Benn's diagrams (Fig. 6), these samples plotted together at a distance from the others.  
562 Such convergence suggests that the elephant carcass, the other faunal remains and the  
563 organic material, deposited on unit UA4, were subjected to the same processes.

564 Far from the isotropic corner in the Benn's diagram these two samples from Area  
565 A plotted almost in between the linear and planar extremes, with the elephant sample  
566 showing a more planar fabric. When the results published by Bertran et al. (1997) and  
567 Lenoble and Bertran (2004) from observations of fabrics in modern subaerial slope  
568 deposits were used as a reference, the two samples aggregated well within the cluster  
569 of runoff process. Yet they still plotted at the extreme margins of debris flow and  
570 relatively distant from the linear corner.

571 This result is consistent with the exposure of unit UA4 to overland water-laden  
572 processes that occurred before the flood event UA3/UB4 (Karkanas et al., this vol-  
573 ume). Notably, the erosive nature of low-energy processes triggered by rain-water has  
574 been observed on lacustrine floodplains, and is associated with anisotropic patterns  
575 in autochthonous assemblages (Cobo-Sánchez et al., 2014; Domínguez-Rodrigo et al.,  
576 2014c; García-Moreno et al., 2016).

577 On the other hand, the fabric of the UA3c sample, being similar to those of the  
578 UB4c sub-samples (Figs. 5 and 6), supports the stratigraphic correlation between these  
579 units across the two investigated areas. The fabric analysis suggests that the UA3/UB4  
580 process can be categorized as a flood event, which falls in the spectrum between debris  
581 and hyperconcentrated flow. Indeed, random distribution and orientation of clasts is ex-  
582 pected for debris flows, except at flow margins, where preferential orientation and clus-  
583 ters of clasts have been observed (Pierson, 2005). Eventually, such flood would have  
584 had the power to significantly reorient elements of the elephant carcass and slightly  
585 displace them.

586 Unlike bones with a tubular shape (i.e., long bones), ribs and vertebrae are prone  
587 to orient preferentially under high energy processes, less likely under low energy pro-  
588 cesses (Domínguez-Rodrigo and García-Pérez, 2013; Domínguez-Rodrigo et al., 2014c).  
589 Interestingly, whereas some of the ribs share the same preferential orientation with the  
590 long bones, others are oriented NW/SE. However, a NW/SE orientation could be con-

591 sistent with a prevalent NE direction of the flow (and vice-versa), since long bones  
592 could roll orthogonally to the flow direction (Voorhies, 1966).

593 On the other hand, a higher energy flood would lead to an under-representation  
594 of most cancellous grease-bearing bones, which are prone to be easily transported by  
595 water induced processes (Voorhies, 1966). Yet several carpals, tarsals, metapodials,  
596 phalanges, ribs and vertebrae are present and in close spatial association with the ele-  
597 phant cranium and other skeletal elements.

598 The presence of many of the skeletal elements suggests that the elephant carcass  
599 was not subjected to high energy processes. Thus, we can assume that relatively low  
600 energy overland flows slightly reworked and oriented the exposed elements of the  
601 already dismembered (and probably already marginally displaced) elephant carcass,  
602 which mostly preserves close anatomical associations, but not anatomical connections.

603 In Area B, two sub-samples from the same stratigraphic unit were analysed, accord-  
604 ing to the different methods used for recording the orientation (dip and strike) of the  
605 finds (i.e., 'clock' vs. compass), mostly faunal remains, wood fragments and lithic arte-  
606 facts. Due to the different shapes of the two distributions (Figs. 4d,e), test statistics re-  
607 ported contrasting results (Tab. 3). Indeed, the clock system, recording non-continuous  
608 circular data, tends to produce a distribution more subject to show a multimodal shape  
609 when the distribution is actually uniform. However, the three-dimensional Woodcock  
610 (Fig. 5) and Benn (Fig. 6) diagrams agreed upon assessing the randomness of the sam-  
611 ples. Despite minor differences between the two samples, both plotted with the UA3c  
612 sample in the reference range of debris flows.

### 613 5.2. *Vertical distribution*

614 As for the vertical distribution, we assume that mass wasting processes, such as  
615 debris or hyperconcentrated flows, would predominantly distribute extremely poorly  
616 sorted clasts homogeneously throughout the sequence. Normal or inverse grading can  
617 be observed in such flows (Pierson, 2005). A concentration of unsorted elements in the  
618 proximity of the erosional surface, as well as the absence of any grading, would in turn  
619 suggest an autochthonous assemblage.

620 The lithic assemblage from Area A - the combined sample from units UA3c and

621 UA4 ( $n = 54$ ), composed by a few debitage products and a relatively high number of  
622 debris/chips and retouch waste products (Tab. 2) - plotted predominantly in the prox-  
623 imity of the erosional surface created by the UA3/UB4 event. The faunal remains  
624 from unit UA3c resemble the distribution of the archaeological assemblage as a whole;  
625 whereas the ones from the underlying unit UA4 match the vertical distribution of the  
626 elephant (Fig. 7).

627 Overall, the material recovered from unit UA3c did not show any grading and  
628 mainly plotted at the bottom of the unit, thus consistent with the hypothesis of an  
629 autochthonous assemblage.

630 In Area B, two samples from units UB4c ( $n = 1243$ ) and UB5a ( $n = 101$ ) re-  
631 spectively, were analysed (Tab. 2), for quantifying the minimum orthogonal distance  
632 of each item to the modelled erosional surface (Fig. 3b).

633 The vertical distribution of lithic artefacts and fossils from unit UB4c showed a pre-  
634 dominant peak right at the contact with the erosional surface. Almost 30% of this rich  
635 sample plotted at a distance between 0 and 5 cm from the erosional contact; whereas  
636 the rest gently skewed to the upper part of the unit, up to about 50 cm. The same distri-  
637 bution was observed for all classes of remains, suggesting no size sorting and an origin  
638 very close to the erosional surface (Fig. 8b).

639 The density distribution of the sample from the underlying UB5a unit (Fig. 8a)  
640 globally indicates a more constrained vertical displacement of remains (within 30 cm  
641 below the erosional surface). Whereas lithic artefacts and fossils mostly plot right at  
642 the contact and just below it, a few debris/chips and faunal remains were found lower  
643 in the sequence. No size sorting was observed, but, notably, lithic cores are absent and  
644 the debris/chip distribution is wider than the distribution of the few flakes and tools.

645 Field observations of cracks in the clayey UB5a unit testify shrinking and swelling  
646 during wetting and drying cycles (Karkanas et al., this volume), which suggests that  
647 vertical displacement of some small lithics and fossil fragments at lower depths with  
648 respect to the UB5a/4c contact probably resulted from clay desiccation.

649 Likewise, [Lenoble and Bertran \(2004\)](#) documented up to 30 cm vertical dispersion  
650 and frequent vertical dip of artefacts from the marshy silty clay of the Croix-de-Canard  
651 site, sector 3.

652 Furthermore, a recent experimental study of animal trampling in water saturated  
653 substrates reported negative correlation with artefact size, significant inclination and  
654 greater vertical displacement than any former work: a maximum between 16 and  
655 21 cm, with a mean of about 6 cm ([Eren et al., 2010](#)).

656 The fact that the majority of the remains from units UB4c and UB5a plotted at  
657 or very close to the contact between these two layers, the relatively high percentage  
658 of lithics in both units, as well as the absence of size sorting or grading, suggest au-  
659 tochthonous assemblages, deposited in UB5a and subsequently eroded *in situ* by the  
660 UA3/UB4 flood event.

661 *5.3. Point pattern analysis*

662 The hypothesis that in both areas the lithic and faunal assemblages were primarily  
663 deposited *in situ* and were subsequently somewhat reworked by a low energy flood,  
664 was further explored by means of point pattern analysis.

665 We assumed that a completely random spatial distribution of the lithic artefacts  
666 and faunal remains would suggest an allochthonous origin and subsequent transport to  
667 the site by the action of a random massive process, such as debris flow. Nevertheless,  
668 clustering of artefacts is not necessary evidence for human presence. Aggregation or  
669 segregation patterns could be produced by a range of biotic and/or natural processes.  
670 Human activities, topography and physical obstructions alike could trigger spatial ag-  
671 gregation.

672 The three-dimensional distribution of lithic artefacts from unit UA3c shows signif-  
673 icant clustering for values of  $r$  between 35 and 65 cm. Lithic artefacts occur relatively  
674 close to the skeletal elements of the elephant, mostly about 20 cm apart and not more  
675 than 50 cm apart ([Fig. 9](#)). The richest cluster of about 20 lithic artefacts is located SW  
676 of the cranium, close to the right femur and the scatter of ribs and vertebrae.

677 Considering the prevalent NE orientation of the elephant bones and the other faunal  
678 remains from UA4, it is not unlikely that a SW/NE oriented flood could have been  
679 responsible for the observed accumulation SW of the elephant cranium, which would  
680 have represented an important obstruction to the flow. A similar case of clustering of  
681 small remains, apparently dammed by a long elephant tusk, has also been observed at

682 Castel di Guido ([Boschian and Saccà, 2010](#)).

683 As mentioned above, whereas fairly random fabric and spatial distribution of coarse  
684 clasts are observed at the centre of modern debris flow deposits, preferential orientation  
685 and clustering may occur at the margin of the flood ([Pierson, 2005](#)). Yet the fabric  
686 analysis of the UA3c sample shows a random distribution, which falls within the range  
687 of debris flow (Fig. 6), and the pair correlation function (Fig. 9b) suggests significant  
688 clustering of lithic artefacts at relatively small scale: a pattern less likely to be produced  
689 by a large scale massive process such as a debris flow. Moreover, clusters of lithic  
690 artefacts occur as well in areas with less density of elephant bones.

691 Small scale clustering; proximity to the elephant remains and the erosional surface;  
692 absence of spatial size sorting and, on the contrary, the presence of a relatively high  
693 number of lithic debris/chips associated with some flakes and tools; close anatomical  
694 spatial association of the elephant skeletal elements, slightly displaced and preferen-  
695 tially oriented: these lines of evidences support the hypothesis of an autochthonous  
696 primary deposition, subject to localised minor reworking.

697 A similar pattern can be observed in Area B, where a first set of spatial statistics  
698 confirmed that the inhomogeneous density of remains from unit UB4c (Fig. 10a) is  
699 not completely explained by the covariate effect of the underlying complex topography  
700 created by the erosional event UA3/UB4 (Fig. 3b).

701 Thus, we explored the relative spatial interaction between the UB4c and the un-  
702 derlying UB5a samples. We assumed that complete spatial randomness of the two  
703 independent depositional processes would occur in case of an exogenous origin and  
704 transportation of the UB4c assemblage. The hypothesis of an autochthonous original  
705 deposition of the faunal and lithic assemblages on the UB5a unit, subsequently eroded  
706 *in situ* by a relatively high energy flood (UB4c), was tested by cross-pattern spatial  
707 correlation functions (Figs. 10d,e). Whereas the two samples are vertically adjacent to  
708 the erosional surface (Fig. 8), on the horizontal plane they are both more segregated  
709 than expected for a random distribution.

710 Moreover, for the UB4c sample, an unsorted particle size spatial distribution was  
711 confirmed (Fig. 11). The occurrence in the same place of small and large classes of  
712 remains suggests that post-depositional processes, such as water winnowing, have not

713 severely affected the assemblage. Hyperconcentrated flows would have dumped mate-  
714 rial on the lake margin. In this way, particles would have been frozen and deposited *en*  
715 *mass*. Hence their non-sorted spatial distribution.

716 On the other hand, the extraordinary preservation and number of mint to sharp,  
717 unsorted lithic artefacts from the UB4c unit; their density, positively correlated to the  
718 topography, and significantly segregated from the underlying distribution of remains;  
719 the vertical proximity of both assemblages from UB4c and UB5a to the erosional sur-  
720 face; as well as the random orientation pattern of the former, suggest that significant  
721 displacement of materials due to the erosional event can be excluded.

722 The faunal and lithic assemblages from unit UB4c therefore most likely derived  
723 from the local erosion of exposed mudflat areas (UB5a layer) and have been slightly  
724 redistributed by the same flood event that capped the elephant in Area A.

725 Further evidence that the recovered assemblage has not undergone substantial re-  
726 working and has retained its original characteristics would come from the refitting  
727 analysis, currently in progress. To date, 4 bone refits have been found in Area B:  
728 three from unit UB4c, respectively at 4.771, 0.048 and 0.012 m distance; and one  
729 between two mammal bone fragments from units UB4c and UB5a, at a very short dis-  
730 tance (0.086 m). Interestingly, one of the elements of the most distant refit (a *Dama*  
731 *sp.* mandibular fragment) shows traces of carnivore gnawing (Konidaris et al., this  
732 volume).

733 In conclusion, multiple lines of evidence suggest that the erosional event UB4/UA3  
734 represents a relatively low-energy process in the continuum between debris and hyper-  
735 concentrated flow, which would have locally reworked at a small scale the already  
736 exposed or slightly buried and spatially associated lithic and faunal assemblages.

737 Although the UB4/UA3 process represents a snapshot of a relatively short frame of  
738 time, inferences about the use of space by human groups, in terms of knapping episodes  
739 and butchering activities, are unreliable in light of the current information.

740 The spatial pattern observed at the site is indeed the result of the last in a palimpsest  
741 of spatial processes. Whereas the erosional event represented by the debris/hyperconcentrated  
742 flow UA3/UB4 caps the sequence and preserves the record, little is known about the  
743 eroded underlying occupational horizon.

744     However, whereas hunting or scavenging is still an unsolved matter of debate, con-  
745     sidering the bone fragmentation rate, the density of lithic debris/chips, the number of  
746     processed bones and their spatial density and association, it is likely that the assemblage  
747     represents a complex palimpsest of locally repeated events of hunting/scavenging and  
748     exploitation of lake shore resources.

749     More data from high resolution excavations in the coming years would allow us to  
750     refine the coarse-grained spatio-temporal resolution of our inferences about past human  
751     behaviour at Marathousa 1.

752     **6. Conclusions**

753     At the Middle Pleistocene open-air site of Marathousa 1 a partial skeleton of a  
754     single individual of *Elephas (Palaeoloxodon) antiquus* was recovered in stratigraphic  
755     association with a rich and consistent lithic assemblage and other vertebrate remains.  
756     Cut-marks and percussion marks have been identified on the elephant and other mam-  
757     mal bones excavated at the site. The main find-bearing horizon represents a secondary  
758     depositional process in a lake margin context.

759     Understanding the site formation processes is of primary importance in order to  
760     reliably infer hominin exploitation of the elephant carcass and other animals. To meet  
761     this aim, we applied a comprehensive set of multivariate and multiscale spatial analyses  
762     in a taphonomic framework.

763     Results from the fabric, vertical distribution and point pattern analyses are consis-  
764     tent with a relatively low-energy erosional process slightly reworking at a small scale  
765     an exposed (or slightly buried) and consistent scatter of lithic artefacts and faunal re-  
766     mains. These results are in agreement with preliminary taphonomic observations of the  
767     lithic artefacts (Tourloukis et al., this volume) and the faunal remains (Konidaris et al.,  
768     this volume), which also indicate minor weathering and transportation. Our analyses  
769     show that multiple lines of evidence support an autochthonous origin of the lithic and  
770     faunal assemblages, subject to minor post-depositional reworking. Human activities  
771     therefore took place on-site, during an as of yet uncertain range of time.

772      **Acknowledgements**

773      This research is supported by the European Research Council (ERC StG PaGE  
774      283503) awarded to K. Harvati. We are grateful to the Municipality of Megalopolis,  
775      the authorities of the Region of Peloponnese, and the Greek Public Power corporation  
776      (ΔΕΗ) for their support. We also thank Julian Bega and all the participants in the PaGE  
777      survey and excavation campaigns in Megalopolis for their indispensable cooperation.

778      **References**

- 779      Anderson, K. L., Burke, A., 2008. Refining the definition of cultural levels at Karabi  
780      Tamchin: a quantitative approach to vertical intra-site spatial analysis. *Journal of*  
781      *Archaeological Science* 35 (8), 2274–2285.
- 782      Baddeley, A., Chang, Y.-M., Song, Y., Turner, R., 2012. Nonparametric estimation of  
783      the dependence of a point process on spatial covariates. *Statistics and Its Interface*  
784      5 (2), 221–236.
- 785      Baddeley, A., Rubak, E., Turner, R., 2015. *Spatial Point Patterns: Methodology and*  
786      *Applications with R*. Chapman and Hall/CRC, London.
- 787      Bar-Yosef, O., Tchernov, E., 1972. On the palaeo-ecological history of the site of Ubei-  
788      diya. Vol. 35. Israel Academy of Sciences and Humanities, Jerusalem.
- 789      Benito-Calvo, A., de la Torre, I., 2011. Analysis of orientation patterns in Olduvai  
790      Bed I assemblages using GIS techniques: Implications for site formation processes.  
791      *Journal of Human Evolution* 61 (1), 50 – 60.
- 792      Benito-Calvo, A., Martínez-Moreno, J., Mora, R., Roy, M., Roda, X., 2011. Tram-  
793      pling experiments at cova gran de santa linya, pre-pyrenees, spain: their relevance  
794      for archaeological fabrics of the upper-middle paleolithic assemblages. *Journal of*  
795      *Archaeological Science* 38 (12), 3652 – 3661.
- 796      Benito-Calvo, A., Martínez-Moreno, J., Pardo, J. F. J., de la Torre, I., Torcal, R. M.,  
797      2009. Sedimentological and archaeological fabrics in Palaeolithic levels of the

- 798 South-Eastern Pyrenees: Cova Gran and Roca dels Bous Sites (Lleida, Spain). Journal  
799 of Archaeological Science 36 (11), 2566 – 2577.
- 800 Benn, D., 1994. Fabric shape and the interpretation of sedimentary fabric data. Journal  
801 of Sedimentary Research 64 (4a), 910–915.
- 802 Berman, M., 1986. Testing for spatial association between a point process and another  
803 stochastic process. Applied Statistics 35, 54–62.
- 804 Bernatchez, J. A., 2010. Taphonomic implications of orientation of plotted finds from  
805 Pinnacle Point 13B (Mossel Bay, Western Cape Province, South Africa). Journal of  
806 Human Evolution 59 (3–4), 274 – 288.
- 807 Bertran, P., Hetù, B., Texier, J.-P., Steijn, H. V., 1997. Fabric characteristics of subaerial  
808 slope deposits. Sedimentology 44 (1), 1 – 16.
- 809 Bertran, P., Lenoble, A., Todisco, D., Desrosiers, P. M., Sørensen, M., 2012. Particle  
810 size distribution of lithic assemblages and taphonomy of Palaeolithic sites. Journal  
811 of Archaeological Science 39 (10), 3148 – 3166.
- 812 Bertran, P., Texier, J.-P., 1995. Fabric Analysis: Application to Paleolithic Sites. Journal  
813 of Archaeological Science 22 (4), 521 – 535.
- 814 Boschian, G., Saccà, D., 2010. Ambiguities in human and elephant interactions? sto-  
815 ries of bones, sand and water from castel di guido (italy). Quaternary International  
816 214 (1–2), 3 – 16, geoarchaeology and Taphonomy.
- 817 Carrer, F., 2015. Interpreting intra-site spatial patterns in seasonal contexts: an ethnoar-  
818 chaeological case study from the western alps. Journal of Archaeological Method  
819 and Theory, 1–25.
- 820 Clark, A. E., 2016. Time and space in the middle paleolithic: Spatial structure and  
821 occupation dynamics of seven open-air sites. Evolutionary Anthropology: Issues,  
822 News, and Reviews 25 (3), 153–163.
- 823 Cobo-Sánchez, L., Aramendi, J., Domínguez-Rodrigo, M., 2014. Orientation patterns  
824 of wildebeest bones on the lake masek floodplain (serengeti, tanzania) and their

- relevance to interpret anisotropy in the olduvai lacustrine floodplain. *Quaternary International* 322–323 (0), 277 – 284, the Evolution of Hominin Behavior during the Oldowan-Acheulian Transition: Recent Evidence from Olduvai Gorge and Peninj (Tanzania).
- Diggle, P., 1985. A kernel method for smoothing point process data. *Applied Statistics (Journal of the Royal Statistical Society, Series C)* 34, 138–147.
- Domínguez-Rodrigo, M., Bunn, H., Mabulla, A., Baquedano, E., Uribelarrea, D., Pérez-González, A., Gidna, A., Yravedra, J., Diez-Martin, F., Egeland, C., Barba, R., Arriaza, M., Organista, E., Ansón, M., 2014a. On meat eating and human evolution: A taphonomic analysis of BK4b (Upper Bed II, Olduvai Gorge, Tanzania), and its bearing on hominin megafaunal consumption. *Quaternary International* 322–323, 129–152.
- Domínguez-Rodrigo, M., Bunn, H., Pickering, T., Mabulla, A., Musiba, C., Baquedano, E., Ashley, G., Diez-Martin, F., Santonja, M., Uribelarrea, D., Barba, R., Yravedra, J., Barboni, D., Arriaza, C., Gidna, A., 2012. Autochthony and orientation patterns in Olduvai Bed I: a re-examination of the status of post-depositional biasing of archaeological assemblages from FLK North (FLKN). *Journal of Archaeological Science* 39 (7), 2116 – 2127.
- Domínguez-Rodrigo, M., Cobo-Sánchez, L., Yravedra, J., Uribelarrea, D., Arriaza, C., Organista, E., Baquedano, E., 2017. Fluvial spatial taphonomy: a new method for the study of post-depositional processes. *Archaeological and Anthropological Sciences*, 1–21.
- Domínguez-Rodrigo, M., Diez-Martín, F., Yravedra, J., Barba, R., Mabulla, A., Baquedano, E., Uribelarrea, D., Sánchez, P., Eren, M. I., 2014b. Study of the SHK Main Site faunal assemblage, Olduvai Gorge, Tanzania: Implications for Bed II taphonomy, paleoecology, and hominin utilization of megafauna. *Quaternary International* 322–323, 153–166.
- Domínguez-Rodrigo, M., García-Pérez, A., 07 2013. Testing the accuracy of different

- 853 a-axis types for measuring the orientation of bones in the archaeological and pale-  
854 ontological record. PLoS ONE 8 (7), e68955.
- 855 Domínguez-Rodrigo, M., Uribelarrea, D., Santonja, M., Bunn, H., García-Pérez, A.,  
856 Pérez-González, A., Panera, J., Rubio-Jara, S., Mabulla, A., Baquedano, E., Yrave-  
857 dra, J., Diez-Martín, F., 2014c. Autochthonous anisotropy of archaeological mate-  
858 rials by the action of water: experimental and archaeological reassessment of the  
859 orientation patterns at the olduvai sites. Journal of Archaeological Science 41 (0),  
860 44 – 68.
- 861 Eren, M. I., Durant, A., Neudorf, C., Haslam, M., Shipton, C., Bora, J., Korisettar,  
862 R., Petraglia, M., 2010. Experimental examination of animal trampling effects on  
863 artifact movement in dry and water saturated substrates: a test case from south india.  
864 Journal of Archaeological Science 37 (12), 3010 – 3021.
- 865 García-Moreno, A., Smith, G. M., Kindler, L., Pop, E., Roebroeks, W., Gaudzinski-  
866 Windheuser, S., Klinkenberg, V., 2016. Evaluating the incidence of hydrological pro-  
867 cesses during site formation through orientation analysis. a case study of the middle  
868 palaeolithic lakeland site of neumark-nord 2 (germany). Journal of Archaeological  
869 Science: Reports 6, 82 – 93.
- 870 Gifford-Gonzalez, D., Damrosch, D., Damrosch, D., Pryor, J., Thunen, R., 1985. The  
871 third dimension in site structure: An experiment in trampling and vertical dispersal.  
872 American Antiquity 50 (4), 803–818.
- 873 Giusti, D., Arzarello, M., 2016. The need for a taphonomic perspective in spatial anal-  
874 ysis: Formation processes at the early pleistocene site of pirro nord (p13), apricena,  
875 italy. Journal of Archaeological Science: Reports 8, 235 – 249.
- 876 Harvati, K., Panagopoulou, E., Tourloukis, V., Thompson, N., Karkanas, P., Athanas-  
877 siou, A., Konidaris, G., Tsartsidou, G., Giusti, D., 2016. New middle pleistocene  
878 elephant butchering site from greece. In: Paleoanthropology Society Meeting. At-  
879 lanta, Georgia, pp. A14–A15.

- 880 Hivernel, F., Hodder, I., 1984. Analysis of artifact distribution at ngenym (kenya):  
881 depositional and postdepositional effects. In: Hietala, H., Larson, P. (Eds.), *Intrasite*  
882 *Spatial Analysis in Archaeology*. Cambridge University Press, Ch. 7, pp. 97–115.
- 883 Hodder, I., Orton, C., 1976. *Spatial Analysis in Archaeology. New Studies in Archae-*  
884 *ology*. Cambridge University Press, Cambridge.
- 885 Isaac, G. L., 1967. Towards the interpretation of occupation debris: Some experiments  
886 and observations. *Kroeber Anthropological Society Papers* 37 (37), 31–57.
- 887 Jammalamadaka, S., Sengupta, A., Sengupta, A., 2001. *Topics in Circular Statistics.*  
888 *Series on multivariate analysis*. World Scientific.
- 889 Lenoble, A., 2005. Ruissellement et formation des sites préhistoriques. Référentiel ac-  
890 tualiste et exemple d’application au fossile. Vol. 1363 of *International Series. British*  
891 *Archaeological Report*, Oxford.
- 892 Lenoble, A., Bertran, P., 2004. Fabric of Palaeolithic levels: methods and implications  
893 for site formation processes. *Journal of Archaeological Science* 31 (4), 457 – 469.
- 894 Lenoble, A., Bertran, P., Lacrampe, F., 2008. Solifluction-induced modifications  
895 of archaeological levels: simulation based on experimental data from a modern  
896 periglacial slope and application to French Palaeolithic sites. *Journal of Archaeo-*  
897 *logical Science* 35 (1), 99 – 110.
- 898 López-Ortega, E., Bargalló, A., de Lombera-Hermida, A., Mosquera, M., Ollé, A.,  
899 Rodríguez-Álvarez, X. P., 2015. Quartz and quartzite refits at gran dolina (sierra  
900 de atapuerca, burgos): Connecting lithic artefacts in the middle pleistocene unit of  
901 td10.1. *Quaternary International*, –.
- 902 López-Ortega, E., Rodríguez, X. P., Vaquero, M., 2011. Lithic refitting and movement  
903 connections: the NW area of level TD10-1 at the Gran Dolina site (Sierra de Ata-  
904 puerca, Burgos, Spain). *Journal of Archaeological Science* 38 (11), 3112 – 3121.
- 905 Marwick, B., 2017. Computational reproducibility in archaeological research: Ba-  
906 sic principles and a case study of their implementation. *Journal of Archaeological*  
907 *Method and Theory* 24 (2), 424–450.

- 908 McPherron, S. J., 2005. Artifact orientations and site formation processes from total  
909 station proveniences. *Journal of Archaeological Science* 32 (7), 1003 – 1014.
- 910 Morin, E., Tsanova, T., Sirakov, N., Rendu, W., Mallye, J.-B., Lèveque, F., 2005. Bone  
911 refits in stratified deposits: testing the chronological grain at saint-cesaire. *Journal*  
912 of Archaeological Science 32, 1083–1098.
- 913 Morton, A. G. T., 2004. Archaeological Site Formation: Understanding Lake Margin  
914 Contexts. No. 1211 in BAR International Series. Archaeopress, Oxford.
- 915 Nickel, B., Riegel, W., Schonherr, T., Velitzelos, E., 1996. Environments of coal forma-  
916 tion in the pleistocene lignite at megalopolis, peloponnesus (greece) - reconstruction  
917 from palynological and petrological investigations. *N. Jb. Geol. Palaont. A.* 200,  
918 201–220.
- 919 Nielsen, A. E., 1991. Trampling the archaeological record: an experimental study.  
920 *American Antiquity* 56 (3), 483–503.
- 921 Ohser, J., 1983. On estimators for the reduced second moment measure of point pro-  
922 cesses. *Mathematische Operationsforschung und Statistik, series Statistics* 14, 63–  
923 71.
- 924 Organista, E., Domínguez-Rodrigo, M., Yravedra, J., Uribelarrea, D., Arriaza, M. C.,  
925 Ortega, M. C., Mabulla, A., Gidna, A., Baquedano, E., 2017. Biotic and abiotic pro-  
926 cesses affecting the formation of {BK} level 4c (bed ii, olduvai gorge) and their bear-  
927 ing on hominin behavior at the site. *Palaeogeography, Palaeoclimatology, Palaeo-  
928 ecology*, –.
- 929 Orton, C., 1982. Stochastic process and archaeological mechanism in spatial analysis.  
930 *Journal of Archaeological Science* 9 (1), 1 – 23.
- 931 Panagopoulou, E., Tourloukis, V., Thompson, N., Athanassiou, A., Tsartsidou, G.,  
932 Konidaris, G., Giusti, D., Karkanas, P., Harvati, K., 2015. Marathousa 1: a new mid-  
933 dle pleistocene archaeological site from greece. *Antiquity Project Gallery* 89 (343).

- 934 Petraglia, M. D., Nash, D. T., 1987. The impact of fluvial processes on experimen-  
935 tal sites. In: Nash, D. T., Petraglia, M. D. (Eds.), Natural formation processes and  
936 the archaeological record. Vol. 352 of International Series. British Archaeological  
937 Reports, Oxford, pp. 108–130.
- 938 Petraglia, M. D., Potts, R., 1994. Water flow and the formation of early pleistocene  
939 artifact sites in olduvai gorge, tanzania. Journal of Anthropological Archaeology  
940 13 (3), 228 – 254.
- 941 Pierson, T. C., 2005. Distinguishing between debris flows and floods from field evi-  
942 dence in small watersheds. Usgs numbered series, U.S. Geological Survey.
- 943 R Core Team, 2016. R: A Language and Environment for Statistical Computing. R  
944 Foundation for Statistical Computing, Vienna, Austria.
- 945 Rick, J. W., 1976. Downslope movement and archaeological intrasite spatial analysis.  
946 American Antiquity 41 (2), 133–144.
- 947 Ripley, B., 1977. Modelling spatial patterns. Journal of the Royal Statistical Society,  
948 series B 39, 172–212.
- 949 Ripley, B., 1988. Statistical inference for spatial processes. Cambridge University  
950 Press.
- 951 Ripley, B. D., 1976. The second-order analysis of stationary point processes. Journal  
952 of Applied Probability 13 (2), 255–266.
- 953 Ripley, B. D., 1981. Spatial Statistics. John Wiley and Sons, New York.
- 954 Schick, K. D., 1984. Processes of paleolithic site formation: an experimental study.  
955 Ph.D. thesis, University of California, Berkeley.
- 956 Schick, K. D., 1986. Stone Age sites in the making: experiments in the formation  
957 and transformation of archaeological occurrences. Vol. 319 of International Series.  
958 British Archaeological Reports, Oxford.

- 959 Schick, K. D., 1987. Modeling the formation of early stone age artifact concentrations.  
960 Journal of Human Evolution 16, 789–807.
- 961 Schiffer, M. B., 1972. Archaeological context and systemic context. American Antiquity 37 (2), 156–165.
- 963 Schiffer, M. B., 1983. Toward the identification of formation processes. American Antiquity 48 (4), 675–706.
- 965 Schiffer, M. B., 1987. Formation processes of the archaeological record. University of New Mexico Press, Albuquerque.
- 967 Shackley, M. L., 1978. The behaviour of artefacts as sedimentary particles in a fluvial environment. Archaeometry 20 (1), 55–61.
- 969 Sisk, M. L., Shea, J. J., 2008. Intrasite spatial variation of the omo kibish middle stone age assemblages: Artifact refitting and distribution patterns. Journal of Human Evolution 55 (3), 486 – 500, paleoanthropology of the Kibish Formation, Southern Ethiopia.
- 973 Sánchez-Romero, L., Benito-Calvo, A., Pérez-González, A., Santonja, M., 12 2016. Assessment of accumulation processes at the middle pleistocene site of ambrona (soria, spain). density and orientation patterns in spatial datasets derived from excavations conducted from the 1960s to the present. PLOS ONE 11 (12), 1–27.
- 977 Todd, L., Stanford, D., 1992. Application of conjoined bone data to site structural studies. In: Hofman, J., Enloe, J. (Eds.), Piecing Together the Past: Applications of Refitting Studies in Archaeology. Vol. 578 of International Series. BAR, Oxford, pp. 21–35.
- 981 van Vugt, N., de Bruijn, H., van kolfschoten, M., Langereis, C. G., 2000. Magneto- and cyclostratigraphy and mammal-fauna's of the pleistocene lacustrine megalopolis basin, peloponnesos, greece. Geologica Ultrajectina 189, 69–92.
- 984 Vaquero, M., Bargalló, A., Chacón, M. G., Romagnoli, F., Sañudo, P., 2015. Lithic recycling in a middle paleolithic expedient context: Evidence from the abric romaní

- 986 (capellades, spain). Quaternary International 361, 212 – 228, the Origins of Recy-  
987 cling: A Paleolithic Perspective.
- 988 Vaquero, M., Chacón, M. G., García-Antón, M. D., de Soler, B. G., Martínez, K.,  
989 Cuartero, F., 2012. Time and space in the formation of lithic assemblages: The  
990 example of Abric Romaní Level J. Quaternary International 247 (0), 162 – 181,  
991 <ce:title>The Neanderthal Home: spatial and social behaviours</ce:title>.
- 992 Villa, P., 1982. Conjoinable pieces and site formation processes. American Antiquity  
993 47 (2), 276–290.
- 994 Villa, P., 1990. Torralba and aridos: elephant exploitation in middle pleistocene spain.  
995 Journal of Human Evolution 19 (3), 299 – 309.
- 996 Villa, P., Courtin, J., 1983. The interpretation of stratified sites: A view from under-  
997 ground. Journal of Archaeological Science 10 (3), 267–281.
- 998 Voorhies, M., 1966. Taphonomy and population dynamics of an early pliocene verte-  
999 brate fauna, knox county, nebraska. Ph.D. thesis, University of Wyoming.
- 1000 Wood, R. W., Johnson, D. L., 1978. A survey of disturbance processes in archaeologi-  
1001 cal site formation. In: Schiffer, M. B. (Ed.), Advances in archaeological method and  
1002 theory. Vol. 1. Academic Press, Ch. 9, pp. 315–381.
- 1003 Woodcock, N., Naylor, M., 1983. Randomness testing in three-dimensional orientation  
1004 data. Journal of Structural Geology 5 (5), 539 – 548.